Nasal endoscopic indocyanine green fluorescence imaging guided surgery for recurrent nasopharyngeal carcinoma

Tingfeng Liang[1], Jing Li[1], Xueyong Hu[1], Yong He[1], Xinting Li[1], Zhenchao Zhu[1], Kunshan He[2], Hongzheng Zhang[1], Chaosheng Yu[1]

Rhinology 64: 5, 0 - 0, 2026
https://doi.org/10.4193/Rhin25.558

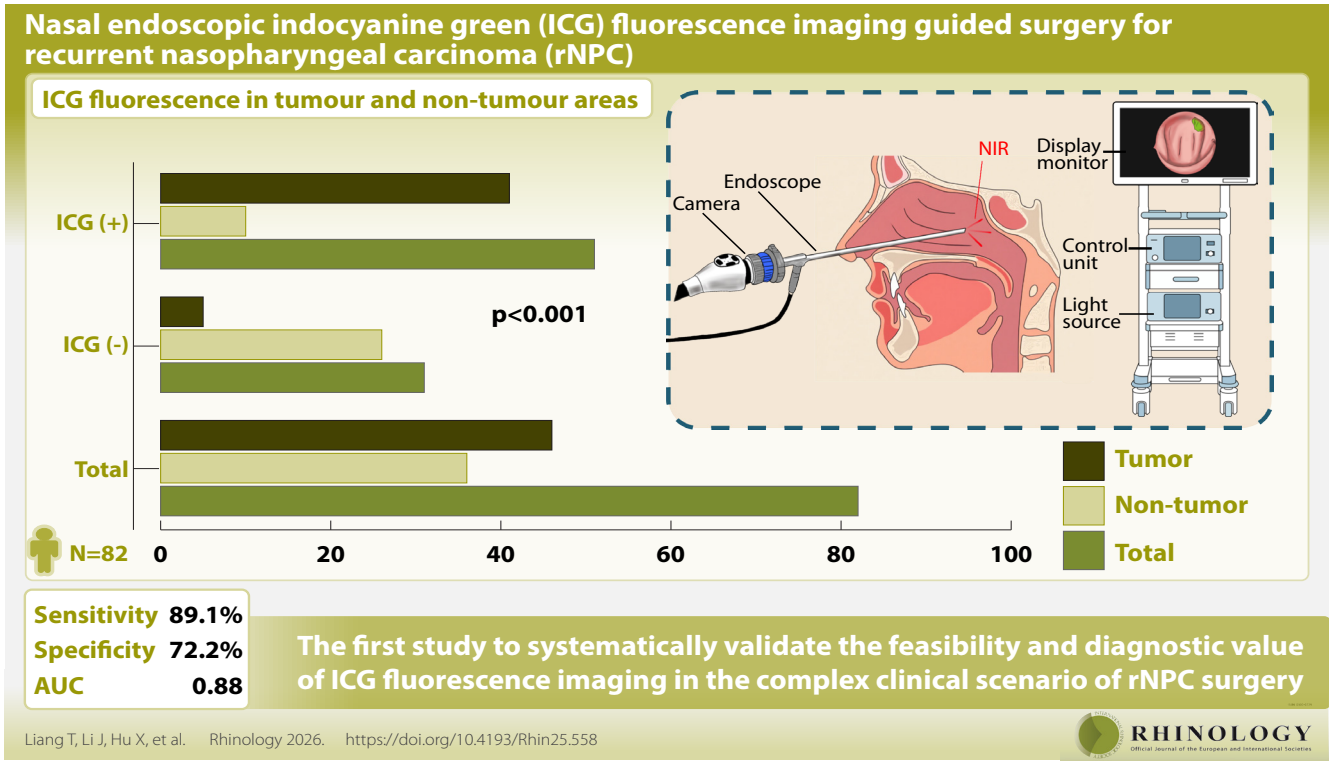

Abstract

Introduction: To evaluate the feasibility and diagnostic value of indocyanine green (ICG) fluorescence imaging in the surgical treatment of recurrent nasopharyngeal carcinoma (rNPC).

Methodology: A retrospective analysis was conducted on clinical data of patients who presented to our department between January 2024 and January 2026, and underwent endoscopic surgery guided by ICG fluorescence imaging system intraoperatively. These patients had previously received radiotherapy for NPC and were found to have suspected recurrence during follow-up examinations. ICG fluorescent agent was administered preoperatively or intraoperatively, and tumours were resected under real-time fluorescence endoscopic monitoring. The fluorescence imaging effects of the tumours and the pathological results of fluorescence-positive lesions were recorded and analysed.

Results: This study included 82 patients with suspected recurrence on preoperative evaluation who underwent ICG fluorescence imaging. Patients were stratified based on pathological findings into tumour group (n=46) and non-tumour group (n=36). Statistical analysis demonstrated a significant correlation between ICG fluorescence localization and pathological diagnosis. The sensitivity of ICG for tumour detection was 89.1%, specificity was 72.2%, positive predictive value was 80.4%, negative predictive value was 83.9%, and overall accuracy was 81.7%. ROC curve analysis yielded an area under the curve (AUC) of 0.88 for ICG fluorescence in distinguishing tumours.

Conclusions: This study is the first to systematically validate the feasibility and diagnostic value of ICG fluorescence imaging in the complex clinical scenario of rNPC surgery, providing a new tool to improve the radicality and safety of surgery for rNPC.

Key words: indocyanine green (ICG), fluorescence imaging, recurrent nasopharyngeal carcinoma (rNPC)

Introduction

Nasopharyngeal carcinoma (NPC) is a malignant tumour originating from the epithelium of the nasopharynx, characterized by distinct geographical and ethnic distribution patterns, with a high incidence in southern China, Southeast Asia, and North Africa [1]. Radiotherapy is the primary treatment modality for NPC. Although multimodal therapy has significantly improved the survival rate of patients with nasopharyngeal carcinoma, approximately 10%–20% of patients still develop local recurrence or distant metastasis after treatment [2].

Recurrent nasopharyngeal carcinoma (rNPC) is defined as a disease in which primary nasopharyngeal carcinoma completely regresses after treatment and then reappears more than six months after the completion of chemoradiotherapy, with recurrence confirmed by biopsy [3]. The main treatment modalities for recurrent nasopharyngeal carcinoma include re-irradiation, surgical resection, chemotherapy, and emerging immunotherapies [4–6]. However, the vast majority of rNPC cases are associated with radioresistance, resulting in low sensitivity of tumour cells to re-irradiation, and most local recurrences occur within high-dose radiation regions. Furthermore, the normal tissues adjacent to the tumour have already been exposed to high-dose radiation from the previous course of treatment, resulting in a high incidence of complications from re-irradiation, which severely impairs patients' quality of life and may even be life-threatening [4]. Existing research has confirmed that in patients with resectable locally recurrent nasopharyngeal carcinoma, the surgical group achieves a markedly better 3-year overall survival (OS) rate compared to the re-irradiation group (85.8% vs. 68.0%), along with a dramatically lower rate of severe late complications [7].

The key to surgical treatment of recurrent nasopharyngeal carcinoma lies in the surgeon's meticulous visual identification of the boundary between tumour and normal tissue, ensuring negative pathological results at both the tumour base and surgical margins [8]. Radical surgery is highly dependent on achieving negative intraoperative margins (R0 resection). However, prior radiotherapy leads to tissue fibrosis, obliteration of anatomical landmarks, and tumour boundaries that are "invisible to the naked eye", resulting in an R0 resection rate of only 60–70% in rNPC [9]. Furthermore, during endonasal endoscopic surgery, the surgeon's localization of the lesion and determination of its margins are subject to subjective factors, which can lead to missed microscopic disease at the resection margins and compromise the patient's long-term quality of life. Excessive tumour resection may result in exposure of critical structures such as the skull base or internal carotid artery, potentially leading to irreversible consequences. This bottleneck urgently requires breakthroughs through intraoperative real-time visualization technologies.

Indocyanine green (ICG) is a fluorescent contrast agent approved by the U.S. Food and Drug Administration (FDA) in 1959 for clinical use; initially, it was primarily employed for liver function assessment and fundus fluorescein angiography [10–12]. Because intravenously administered ICG is eliminated exclusively by the liver, it was first introduced and has been used for decades to assess human liver function, demonstrating an excellent safety profile [13]. ICG exhibits an absorption peak near 780–810 nm and an emission peak at 810–820 nm [14,15]. Since the emission wavelength of indocyanine green lies within the near-infrared optical window, its fluorescence signal achieves an effective penetration depth of approximately 5–10 mm in soft tissue [16]. After intravenous administration, ICG has a very short half-life of 3-4 minutes and is cleared exclusively by the liver [17]. The relatively hydrophobic ICG molecules bind rapidly and almost completely to serum proteins [15]. Protein binding reduces aggregation, increases brightness (i.e., quantum yield) by more than threefold, and increases the effective hydrodynamic diameter to that of the bound protein [18], thereby enabling detection by the fluorescence endoscopy receiver upon excitation with near-infrared light. In oncologic surgery, ICG is not a typical "tumour-specific probe"; rather, it functions via the abnormal permeability of tumour vasculature or differences in excretory function between tumour and surrounding tissues. For example, it has previously been considered that in non-hepatic tumours, ICG fluorescence is enhanced through selective accumulation in tumour tissues resulting from the binding of ICG to high-molecular-weight serum proteins [19]. The enhanced permeability and retention (EPR) effect is considered associated with the accumulation of ICG in tumour cells [20]. In colorectal cancer cell lines, the tumour cell preference of ICG is driven by passive tumour cell targeting, the inherent ability of ICG to bind to cell membranes, and high endocytic activity associated with the disruption of tight connections between tumour cells and tumour tissue [21]. In liver tumours, the ICG-positive portion is associated with the expression of the membrane transporters organic anion transporting polypeptide 1B3 (OATP1B3) and sodium taurocholate co-transporting polypeptide (NTCP) [22,23], both of which are normally expressed in hepatocytes and mediate cellular uptake of ICG in vitro. Furthermore, research indicates that scavenger receptors (SRs) not only promote clathrin receptor upregulation via downstream signalling activation upon binding to the ICG albumin complex, but also directly facilitate ICG transmembrane trafficking through recognition of its hydrophobic moieties, thus enhancing the active cellular uptake of ICG [24].

ICG fluorescence imaging technology has rapidly advanced in the field of surgical oncology, leveraging the unique fluorescence properties of ICG to enable real-time visualization during surgery. In recent years, ICG has been widely applied in the surgical treatment of various cancers, including liver cancer [25], breast cancer [26], gastric cancer [27], colorectal cancer [28], and lung cancer [29], demonstrating significant surgical efficacy and improving surgeons' ability to localize lesions and assess resection margins. For example, ICG fluorescence imaging can be used to

Table 1. Clinical baseline.

Variable	N=82 [a]
Age	57.76(11.25)
Sex	
Male	58(70.7%)
Female	11(29.3%)
Weight	57.67(13.08)
rNPC	46(56.1%)
Non- rNPC	36(43.9%)
rNPC T staging [b]	
T1	2(4.3%)
T2	8(17.4%)
T3	29(63.0%)
T4	7(15.2%)

[a] Mean (SD); N (%). [b] The T staging is based on the TNM staging system of the 9th edition of the AJCC.

Table 2. Summary of ICG injection patterns for 82 patients.

Variable	N=82
Injection time	
Intraoperative only	5
Preoperative+ Intraoperative	77
Preoperative 3h	31
Preoperative 6h	24
Preoperative 12h	22
Preoperative injection dose	
0.5mg/kg	25
0.6mg/kg	33
0.7mg/kg	19

detect primary and secondary hepatic malignancies, with a sensitivity of over 90% [30,31]. In breast cancer, the sensitivity of ICG fluorescence imaging in detecting sentinel lymph nodes ranges from 95% to 100% [32,33]. In ICG fluorescence-guided surgery for colorectal liver metastases, the overall R0 resection rate is up to 92.4%, while the real time evaluation of resection margins yields a sensitivity of 60% and a specificity of 90% [34]. However, there are few reports or relevant clinical studies on the application of ICG fluorescence imaging in endoscopic surgery for recurrent nasopharyngeal carcinoma. We have previously conducted preliminary exploration and case report on the use of indocyanine green fluorescence imaging in the surgical treatment of recurrent nasopharyngeal carcinoma [35]. This retrospective study investigates the application of indocyanine green fluorescence imaging in the surgical management of recurrent nasopharyngeal carcinoma, aiming to evaluate its feasibility and diagnostic value, thereby providing clinical experience to support its further application in endoscopic surgical procedures.

Materials and methods

Clinical data collection

This retrospective study included 82 patients with a history of radiation therapy for nasopharyngeal malignancies, who were admitted to the Department of Otorhinolaryngology Head and Neck Surgery of Zhujiang Hospital, Southern Medical University, from January 2024 to January 2026. Patients were considered to have potential recurrence based on their clinical histories and preoperative assessments, including nasal endoscopy, contrast-enhanced MRI or CT of the nasopharynx, and PET/CT. These patients underwent endoscopic endonasal surgery of the nose and skull base with intraoperative assistance from indocyanine green (ICG) fluorescence imaging system. Clinical baseline data of the patients, including age, sex, body weight, and tumour stage, were collected (Table 1). The ICG-localized positions were recorded from surgical videos and compared with final pathological results to determine whether the target areas were localized and to confirm tumour diagnosis within the localized regions. This study was approved by the Ethics Committee of Zhujiang Hospital, Southern Medical University (Approval No.: 2024-KY-265-01).

Reagents and instruments

Indocyanine green for injection (25 mg/vial), manufactured by Dandong Yichuang Pharmaceutical Co., Ltd., was administered intravenously at a dose based on patient's body weight, according to the strategy outlined in Table 2. Fluorescence imaging was performed using the DPM 4K fluorescence endoscopy system (DPM-H3800), which comprises a control unit, light source, monitor, fluorescence endoscope and other components, and offers both standard and fluorescence modes (Figure 3).

Methods

After admission, patients underwent routine examinations and evaluations; upon exclusion of relevant contraindications to surgery, endoscopic endonasal resection of nasopharyngeal and skull base tumours was scheduled within a limited timeframe. The surgery was performed under general anaesthesia. After adequate exposure of the tumour tissue, the tumour region was examined using a fluorescence endoscopy system. Indocyanine green (ICG) is prone to quenching upon excitation by near-infrared light. If intraoperative fluorescence quenching occurs due to prolonged observation with the fluorescence endoscope, a supplementary injection of ICG at a dose of 2.5 mg per administration is required.

According to a previous case report from our team [35], delayed ICG fluorescence clearance was observed intraoperatively in

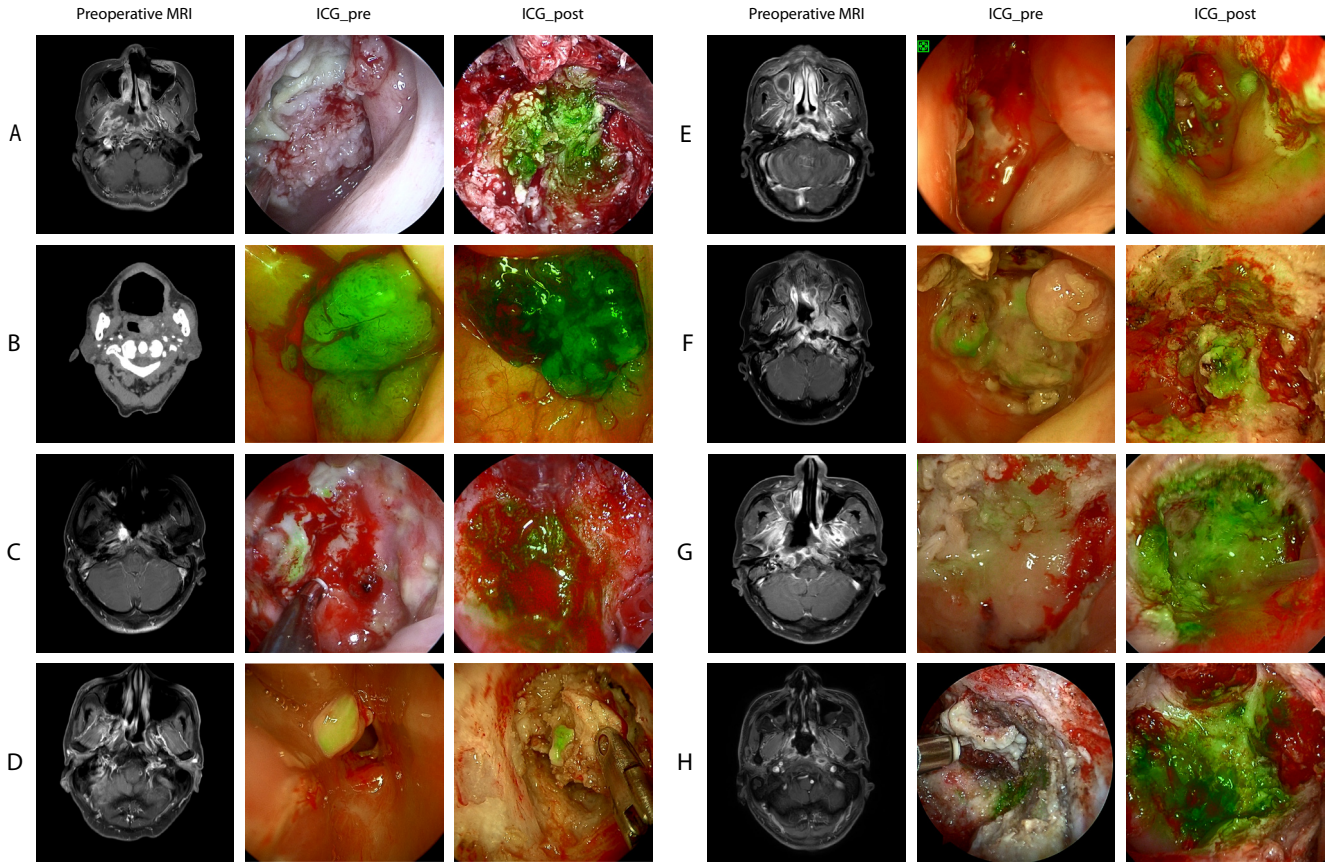

Figure 1. The ICG fluorescence imaging effect of rNPC. A) In case 8 of rNPC patient, preoperative MRI revealed a soft tissue mass in the nasopharynx and the right lateral wall, with heterogeneous and marked enhancement on contrast enhanced scanning. Before intraoperative supplemental ICG injection, no fluorescence was observed; after the booster injection, green fluorescence was visible in the target region. B) In case 11 of rNPC patient with rT2 stage, preoperative contrast-enhanced CT showed soft tissue shadows in the lateral walls of the nasopharynx and oropharynx, with evidence of enhancement. Before intraoperative supplemental ICG injection, intense green fluorescence was already observed. C) In case 12 of rNPC patient, preoperative MRI revealed soft tissue in the right nasopharynx. Before and after intraoperative supplemental ICG injection, stronger fluorescence was observed compared with that of the inferior turbinate. D) In case 19 of rNPC patient with rT2 stage, preoperative MRI showed an enhanced signal at the upper margin of the right posterior naris and the nasopharynx. Before intraoperative supplemental ICG injection, moderate fluorescence was observed; during surgery, due to fluorescence quenching, a supplemental ICG injection was administered, and the tumour was completely resected under ICG fluorescence guidance. E) In case 32 of rNPC patient, preoperative MRI revealed a space occupying lesion in the posterior wall of the nasopharyngeal roof; however, intraoperatively we observed fluorescence at the posterior margin of the nasal septum, and pathological examination confirmed that tumour tissue was also present at that site. Before intraoperative supplemental ICG injection, weak fluorescence was observed compared with that of the inferior turbinate; after supplemental injection, strong fluorescence became visible. F) In case 35 of patient with skull base osteoradionecrosis (sbORN) complicated by rNPC, preoperative MRI showed an irregular soft tissue mass in the left lateral wall and the posterosuperior wall of the nasopharynx, with marked heterogeneous enhancement on contrast enhanced scanning. Intraoperatively, scattered fluorescence was observed in the necrotic area, and pathology confirmed the presence of tumour tissue. G) In case 39 of rNPC patient, preoperative MRI showed marked enhancement of the nasopharyngeal wall. Before intraoperative supplemental ICG injection, weak fluorescence was observed compared with the inferior turbinate, while after supplemental injection, strong and diffuse fluorescence became visible, and pathology confirmed diffuse tumour infiltration. H) In case 41 of rNPC patient, MRI showed uneven thickening of all walls of the nasopharynx with heterogeneous enhancement on contrast enhanced scanning. Before intraoperative supplemental ICG injection, green fluorescence was observed in the necrotic area; after the booster injection, strong and diffuse fluorescence became visible, and pathology confirmed diffuse tumour infiltration.

the nasal septum and inferior turbinate, with a discernible difference in fluorescence intensity compared to that of tumour fluorescence (Figure S1). This phenomenon can serve as an internal control. In patients who have undergone radiotherapy for nasopharyngeal carcinoma, the inferior turbinate is less affected by radiation and is commonly used clinically for skull base

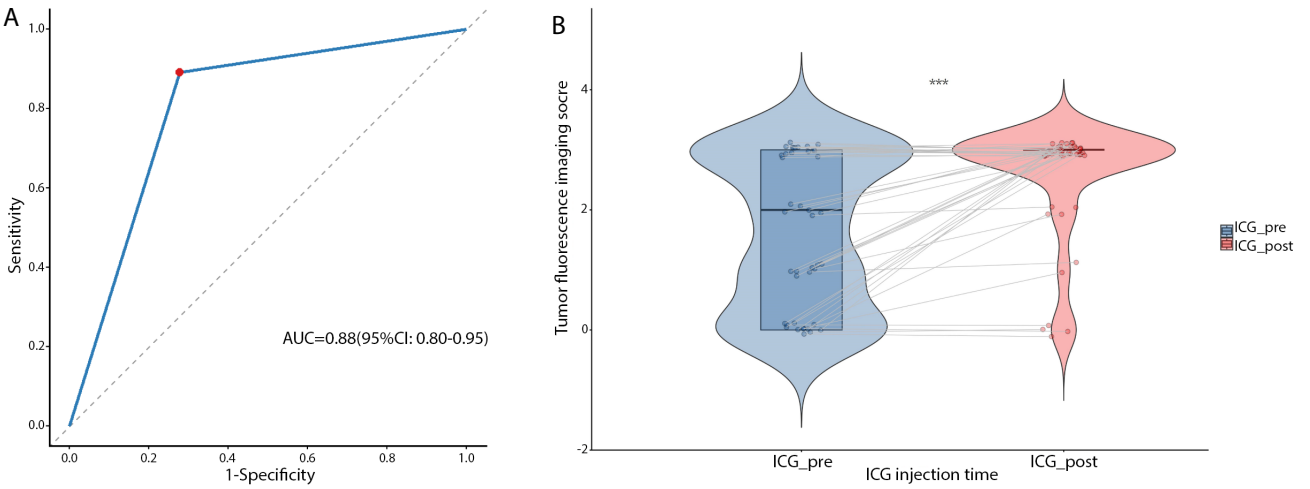

Figure 2. Performance of ICG fluorescence for tumour localization and imaging assessment. A) ROC curve of ICG fluorescence for localizing the target region. B) Comparison of tumour fluorescence imaging scores between preoperative ICG injection (ICG_pre) and intraoperative supplemental ICG injection (ICG_post).

defect reconstruction [36]. Based on this observation, our study employed the inferior turbinate as an in vivo reference tissue for relative evaluation of fluorescence imaging in the target region. Fluorescence in the tumour tissue or target area was compared with that in the inferior turbinate: if tumour fluorescence exceeded inferior turbinate fluorescence, the tumour fluorescence imaging effect was considered strong; if tumour fluorescence was comparable to inferior turbinate fluorescence, the effect was considered moderate; if tumour fluorescence was lower than inferior turbinate fluorescence, the effect was considered weak. Accordingly, the fluorescence visualization effect of the tumour was scored on a 0–3 scale: 0 for no fluorescence, 1 for weak fluorescence, 2 for moderate fluorescence, and 3 for strong fluorescence.

Statistical analysis

Data management, statistical analyses, and generation of statistical figures were conducted using SPSS 26.0 and R 4.5.2. Continuous variables were assessed for normality using the Shapiro-Wilk test: normally distributed data were presented as mean ± standard deviation (x ± s); non-normally distributed data were described as median (interquartile range, M [IQR]). Categorical variables were presented as frequencies (percentages), and comparisons between groups were performed using Pearson's chi-squared test or Fisher's exact test (when the expected frequency in any cell was <5). Sensitivity, specificity, positive predictive value (PPV), negative predictive value (NPV), and accuracy were calculated using standard formulas. Receiver operating characteristic (ROC) curves were generated using the pROC and ggplot2 package, and the area under the curve (AUC) along with its 95% confidence interval (CI) was calculated using DeLong's method. All tests were two-tailed, and a P-value < 0.05 was considered statistically significant.

Results

This study enrolled 82 patients with suspected recurrence of nasopharyngeal carcinoma who underwent ICG fluorescence imaging, comprising 58 males and 24 females. The mean age was 52.76±11.26 years, and the mean body weight was 57.67±13.08 kg (Table 1 for clinical baseline). Among the 82 patients, 5 received ICG injection only intraoperatively, while 77 received ICG both preoperatively and intraoperatively, with varying preoperative injection doses and timing, aiming to explore the injection regimen that achieves better ICG visualization effects (Table 2). Based on pathological results, 46 patients were classified into the tumour group, and 36 patients into the non-tumour group. Comparing the intraoperative ICG fluorescence localization sites with the lesion locations on preoperative MRI, we found that in patients with tumours, ICG fluorescence could localize the target area and guide surgical resection (Figure 1). The raw intraoperative ICG fluorescence images of these tumour patients are available in the additional file.

Pearson's chi-square test revealed a statistically significant correlation between ICG findings and the presence or absence of tumours (P < 0.001, Table 3). Using pathological results as the reference standard, ICG fluorescence demonstrated a sensitivity of 89.1% (41/46), specificity of 72.2% (26/36), PPV of 80.4% (41/51), NPV of 83.9% (26/31), and overall accuracy of 81.7% (67/82). ROC curve analysis indicated that ICG fluorescence had good diagnostic performance in discriminating tumour from non-tumour tissues, with an area under the curve (AUC) of 0.88 (95% CI: 0.80–0.95, Figure 2A), suggesting that ICG fluorescence

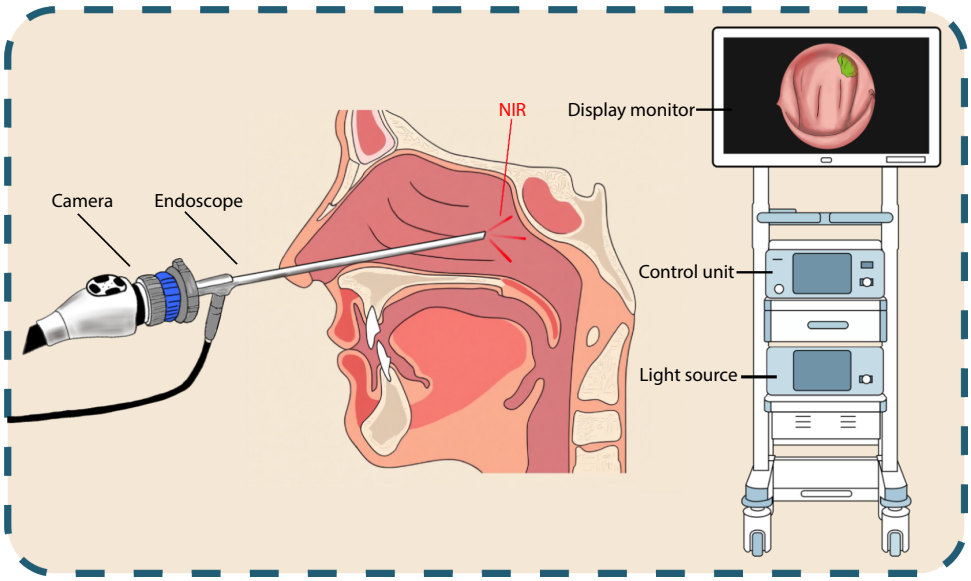

Figure 3. Illustration showing nasal endoscopic indocyanine green fluorescence imaging guided surgery for recurrent nasopharyngeal carcinoma. NIR: near-infrared.

Table 3. Cross-analysis table of ICG fluorescence in tumour and non-tumour areas.

Group	Tumour	Non-Tumour	Total	Statistic	P
ICG (+)	41(89.1%)	10 (27.8%)	51 (62.2%)		
ICG (-)	5 (10.9%)	26 (72.2%)	31 (37.8%)	32.33	<0.001
Total	46 (100.0%)	36 (100.0%)	82 (100.0%)		

has a favourable ability to identify tumours.

Compared with pre-supplementation injection (ICG_pre), tumour fluorescence imaging scores were significantly increased after the supplementary injection (ICG_post) ($P < 0.001$, Tables S1 and S2). Violin plots showed that the overall score distribution shifted toward higher score ranges after the supplementary injection, with both the median and interquartile range notably shifted upward, indicating that intraoperative supplementary injection enhances tumour fluorescence visualization (Figure 2B).

Discussion

This study systematically validated the clinical feasibility and diagnostic efficacy of ICG near-infrared fluorescence imaging in rNPC surgery for the first time in a retrospective cohort, particularly achieving real-time and visual identification of tumour tissue during endoscopic rNPC surgery. Overall, ICG fluorescence showed high sensitivity (89.1%) in tumour localization, indicating its superior detection capability in tumour screening and intraoperative localization. However, its specificity was moderate (72.2%), with approximately 27.8% of non-tumour tissues exhibiting fluorescence, suggesting that ICG fluorescence is not a tumour-specific signal and may be related to factors such as inflammatory response, increased vascular permeability, and tissue oedema. Furthermore, the high positive predictive value (80.4%) indicates that positive ICG fluorescence is highly suggestive of tumour, offering critical guidance for intraoperative decisions such as biopsy acquisition or margin extension. Although its negative predictive value was high (83.9%), this suggests that suspicious areas should not be ignored solely based on negative fluorescence, and a comprehensive judgment combined with imaging and routine pathology is required. This characteristic is consistent with previous observations in gastric and liver cancers: ICG fluorescence is a "strong positive-oriented tool" rather than an "exclusionary diagnostic tool" [37,38]. In summary, ICG fluorescence in the target area has high sensitivity and positive predictive value in tumour identification, but its moderate specificity suggests it can serve as an effective intraoperative auxiliary localization method rather than a replacement for pathological diagnosis.

Our study found that false-positive ICG fluorescence was primarily concentrated in inflammatory lesions. This is highly consistent with Holt's study: increased vascular permeability in inflammatory areas can also lead to ICG leakage and accumulation, but its fluorescence pattern is usually diffuse with blurred boundaries, whereas tumour fluorescence is mostly focal with sharp boundaries [39]. Consequently, we propose the implementation of "fluorescence morphological criteria" for surgeons: 1) focal intense fluorescence with distinct margins: highly sug-

gestive of malignancy;
2) diffuse faint fluorescence with indistinct margins: indicative of inflammation or necrosis.

Although ICG imaging has significant advantages in recurrent nasopharyngeal carcinoma surgery, its inherent limitations must be clearly recognized:
1) Penetration depth limitation: near-infrared light effectively penetrates only 5–10 mm in soft tissue, resulting in limited identification capability for deep infiltrative lesions (such as the sphenoid body and pterygoid base) [40];
2) Non-specific accumulation: inflammation and granulation tissue can also cause false positives (false positive rate of 27.8% in this study), requiring interpretation in combination with pathological diagnosis;
3) Fluorescence quenching: prolonged exposure to white light or intraoperative irrigation can cause signal attenuation, which was effectively mitigated in this study by an "intraoperative supplemental injection of 2.5 mg". However, intraoperative injection of ICG can easily lead to "fluorescence pollution" in the surgical field, and ICG fluorescence in surgical bleeding can cause interference, affecting the judgment of resection margins;
4) Lack of standardized protocols: there is currently no unified specification for injection timing or dosage. In endoscopic endonasal surgery, further clinical studies are still needed to determine the ICG injection method, dosage, and timing to achieve optimal visualization of tumour tissues.

ICG fluorescence imaging technology holds significant clinical application value in the surgical treatment of recurrent nasopharyngeal carcinoma. First, ICG fluorescence imaging significantly enhances the surgeon's ability to delineate tumour boundaries, reducing intraoperative errors and the risk of positive margins, thereby improving the completeness of resection. Second, ICG fluorescence imaging enables real-time intraoperative monitoring, assisting surgeons in promptly identifying and managing potential complications such as vascular injury, thereby further enhancing surgical safety and efficacy. Furthermore, ICG fluorescence imaging can provide immediate postoperative assessment by observing fluorescence activity in the surgical field, allowing for timely detection and management of residual lesions. Future prospective randomized controlled trials are needed to validate its ability to improve recurrence-free survival (RFS) and overall survival (OS), and to promote the development of standardized operating procedures (SOPs), ultimately establishing it as a routine component of precision surgery for nasopharyngeal and skull base tumours.

Conclusion

The application of indocyanine green (ICG) fluorescence imaging in surgery for recurrent nasopharyngeal carcinoma demonstrates its substantial potential and clinical value in complex oncological surgeries. This study provides the first systematic validation of the feasibility and diagnostic value of ICG fluorescence imaging in nasal and skull base surgery, particularly in the complex clinical setting of recurrent nasopharyngeal carcinoma, thereby offering a new tool to improve the radicality and safety of surgical treatment for recurrent nasopharyngeal carcinoma. However, the application of ICG fluorescence imaging in recurrent nasopharyngeal carcinoma still requires further clinical studies and technical optimization to ensure its broad applicability across different clinical settings and its long-term effectiveness.

Acknowledgments

This research was supported by National Natural Science Foundation of China (82573354) and Dean's Fund Program of Zhujiang Hospital of Southern Medical University (yzjj2024ms08).

Author contributions

TL was responsible for data collection and paper writing. XH, JL, YH, XL and ZZ were in charge of patient management. KH provided technical support. HZ, CY are joint corresponding author and responsible for the implementation of the surgery and providing guidance.

Conflict of interest

The authors declare no conflicts of interest.

Funding

National Natural Science Foundation of China (82573354), Dean's Fund Program of Zhujiang Hospital of Southern Medical University (yzjj2024ms08).

References

1. Su ZY, Siak PY, Lwin YY, Cheah SC. Epidemiology of nasopharyngeal carcinoma: Current insights and future outlook. Cancer Metastasis Rev. 2024 Sep 1;43(3):919–39.
2. Chen YP, Chan ATC, Le QT, Blanchard P, Sun Y, Ma J. Nasopharyngeal carcinoma. Lancet. 2019 Jul 6;394(10192):64–80.
3. Stoker SD, van Diessen JNA, de Boer JP, Karakullukcu B, Leemans CR, Tan IB. Current treatment options for local residual nasopharyngeal carcinoma. Curr Treat Options Oncol. 2013 Dec;14(4):475–91.
4. Lee AWM, Ng WT, Chan JYW, et al. Management of locally recurrent nasopharyngeal carcinoma. Cancer Treat Rev. 2019 Sep;79:101890.
5. Ng WT, Soong YL, Ahn YC, et al. International recommendations on reirradiation by intensity modulated radiation therapy for locally recurrent nasopharyngeal carcinoma. Int J Radiat Oncol Biol Phys. 2021 Jul 1;110(3):682–95.
6. Wang D, Liao M, Wu J, et al. Salvage treatments for locally recurrent nasopharyngeal cancer: Systematic review and meta-analysis. Head Neck. 2023 Feb;45(2):503–20.
7. Liu YP, Wen YH, Tang J, et al. Endoscopic surgery compared with intensity-modulated radiotherapy in resectable locally recurrent nasopharyngeal carcinoma: A multicentre, open-label, randomised, controlled, phase 3

trial. Lancet, Oncol. 2021 Mar;22(3):381–90.
8. Li W, Lu H, Wang H, et al. Salvage endoscopic nasopharyngectomy in recurrent nasopharyngeal carcinoma: Prognostic factors and treatment outcomes. Am J Rhinol Allergy. 2021 Jul;35(4):458–66.
9. Daloiso A, Gaudioso P, Vinciguerra A, et al. Margins in oncologic nasopharyngeal surgery: A systematic review with meta-analysis. Acta Otorhinolaryngol Ital. 2025 May;45(2 Suppl 1):S56–70.
10. Cherrick GR, Stein SW, Leevy CM, Davidson CS. Indocyanine green: observations on its physical properties, plasma decay, and hepatic extraction. J Clin Invest. 1960 Apr;39(4):592–600.
11. Arnold JJ, Quaranta M, Soubrane G, Sarks SH, Coscas G. Indocyanine green angiography of drusen. Am J Ophthalmol. 1997 Sep;124(3):344–56.
12. Owens SL. Indocyanine green angiography. Br J Ophthalmol. 1996 Mar 1;80(3):263–6.
13. Hope-Ross M, Yannuzzi LA, Gragoudas ES, et al. Adverse reactions due to indocyanine green. Ophthalmology. 1994 Mar;101(3):529–33.
14. Desmettre T, Devoisselle JM, Mordon S. Fluorescence properties and metabolic features of indocyanine green (ICG) as related to angiography. Surv Ophthalmol. 2000;45(1):15–27.
15. Landsman ML, Kwant G, Mook GA, Zijlstra WG. Light-absorbing properties, stability, and spectral stabilization of indocyanine green. J Appl Physiol. 1976 Apr;40(4):575–83.
16. Vahrmeijer AL, Hutteman M, van der Vorst JR, van de Velde CJH, Frangioni JV. Image-guided cancer surgery using near-infrared fluorescence. Nat Rev Clin Oncol. 2013 Sep;10(9):507–18.
17. Chon B, Ghann W, Uddin J, Anvari B, Kundra V. Indocyanine green (ICG) fluorescence is dependent on monomer with planar and twisted structures and inhibited by H-aggregation. Int J Mol Sci. 2023 Aug 22;24(17):13030.
18. Yoneya S, Saito T, Komatsu Y, Koyama I, Takahashi K, Duvoll-Young J. Binding properties of indocyanine green in human blood. Invest Ophthalmol Vis Sci. 1998 Jun;39(7):1286–90.
19. Holt D, Okusanya O, Judy R, et al. Intraoperative near-infrared imaging can distinguish cancer from normal tissue but not inflammation. Multhoff G, editor. PLoS ONE. 2014 Jul 29;9(7):e103342.
20. Maeda H, Nakamura H, Fang J. The EPR effect for macromolecular drug delivery to solid tumors: Improvement of tumor uptake, lowering of systemic toxicity, and distinct tumor imaging in vivo. Advanced Drug Delivery Reviews. 2013 Jan;65(1):71–9.
21. Onda N, Kimura M, Yoshida T, Shibutani M. Preferential tumor cellular uptake and retention of indocyanine green for in vivo tumor imaging. Int J Cancer. 2016 Aug 1;139(3):673–82.
22. Ishizawa T, Masuda K, Urano Y, et al. Mechanistic background and clinical applications of indocyanine green fluorescence imaging of hepatocellular carcinoma. Ann Surg Oncol. 2014 Feb;21(2):440–8.
23. Shibasaki Y, Sakaguchi T, Hiraide T, et al. Expression of indocyanine green-related transporters in hepatocellular carcinoma. J Surg Res. 2015 Feb;193(2):567–76.
24. Wang J, Peng X, Wei J, et al. In situ phagocyte-mediated deep tumor penetration assisted by ApoA-1 mimetic peptide-modified silicasome. Nano Today. 2023 Jun 1;50:101864.
25. Jhan CH, Kao WY, Huang YM. Indocyanine green fluorescence imaging-assisted laparoscopic radiofrequency ablation of hepatocellular carcinoma. Clin Gastroenterol Hepatol. 2023 Jun;21(6):A19–20.
26. Bargon CA, Huibers A, Young-Afat DA, et al. Sentinel lymph node mapping in breast cancer patients through fluorescent imaging using indocyanine green: the INFLUENCE trial. Ann Surg. 2022 Nov 1;276(5):913–20.
27. Chen QY, Xie JW, Zhong Q, et al. Safety and efficacy of indocyanine green tracer-guided lymph node dissection during laparoscopic radical gastrectomy in patients with gastric cancer: a randomized clinical trial. JAMA Surg. 2020 Apr 1;155(4):300–11.
28. Keller DS, Ishizawa T, Cohen R, Chand M. Indocyanine green fluorescence imaging in colorectal surgery: Overview, applications, and future directions. Lancet Gastroenterol Hepatol. 2017 Oct;2(10):757–66.
29. Quan YH, Oh CH, Jung D, et al. Evaluation of intraoperative near-infrared fluorescence visualization of the lung tumor margin with indocyanine green inhalation. JAMA Surg. 2020 Aug 1;155(8):732–40.
30. Franz M, Arend J, Wolff S, et al. Tumor visualization and fluorescence angiography with indocyanine green (ICG) in laparoscopic and robotic hepatobiliary surgery - valuation of early adopters from Germany. Innov Surg Sci. 2021 Jun;6(2):59–66.
31. Zhou J, Tan Z, Sun B, Leng Y, Liu S. Application of indocyanine green fluorescence imaging in hepatobiliary surgery. Int J Surg. 2024 Dec;110(12):7948.
32. White KP, Sinagra D, Dip F, et al. Indocyanine green fluorescence versus blue dye, technetium-99M, and the dual-marker combination of technetium-99M + blue dye for sentinel lymph node detection in early breast cancer-meta-analysis including consistency analysis. Surgery. 2024 Apr;175(4):963–73.
33. Pitsinis V, Kanitkar R, Vinci A, Choong WL, Benson J. Results of a prospective randomized multicenter study comparing indocyanine green (ICG) fluorescence combined with a standard tracer versus ICG alone for sentinel lymph node biopsy in early breast cancer: The INFLUENCE trial. Ann Surg Oncol. 2024 Dec 1;31(13):8848–55.
34. Achterberg FB, Bijlstra OD, Slooter MD, et al. ICG-fluorescence imaging for margin assessment during minimally invasive colorectal liver metastasis resection. JAMA Netw Open. 2024 Apr 1;7(4):e246548.
35. Liang T, Hu X, Li J, et al. Application of real-time indocyanine green fluorescence imaging in recurrent nasopharyngeal carcinoma surgery. Ann Surg Oncol. 2025 Jun 16;
36. Liu YT, Ren HY, Yuan ZD, et al. Pedicled inferior turbinate-nasal floor and septal mucoperiosteal flap resurfacing for PRNN. Laryngoscope. 2026 Jul;136(7):2971-2978.
37. Piccolo G, Barabino M, Diana M, et al. Application of indocyanine green fluorescence as an adjuvant to laparoscopic ultrasound in minimally invasive liver resection. J Laparoendosc Adv Surg Tech A. 2021 May;31(5):517–23.
38. Chen QY, Xie JW, Zhong Q, et al. Safety and efficacy of indocyanine green tracer-guided lymph node dissection during laparoscopic radical gastrectomy in patients with gastric cancer: A randomized clinical trial. JAMA Surg. 2020 Apr 1;155(4):301–11.
39. Holt D, Okusanya O, Judy R, et al. Intraoperative near-infrared imaging can distinguish cancer from normal tissue but not inflammation. PLOS One. 2014;9(7):e103342.
40. Vahrmeijer AL, Hutteman M, Vorst JR van der, Velde C van de, Frangioni JV. Image-guided cancer surgery using near-infrared fluorescence. Nat Rev Clin Oncol. 2013 Jul 23;10(9):507.

Hongzheng Zhang
Department of Otolaryngology
Head and Neck Surgery
Zhujiang Hospital
Southern Medical University
Guangzhou
China

E-mail: zhang_hongzheng@yeah.net

Chaosheng Yu
Department of Otolaryngology
Head and Neck Surgery
Zhujiang Hospital
Southern Medical University
Guangzhou
China

E-mail: ycs_9982@163.com

Tingfeng Liang[1], Jing Li[1], Xueyong Hu[1], Yong He[1], Xinting Li[1], Zhenchao Zhu[1], Kunshan He[2], Hongzheng Zhang[1], Chaosheng Yu[1]

[1] Department of Otolaryngology Head and Neck Surgery, Zhujiang Hospital, Southern Medical University, Guangzhou, China

[2] CAS Key Laboratory of Molecular Imaging, Beijing Key Laboratory of Molecular Imaging, Institute of Automation, Chinese Academy of Sciences, Beijing, China

Rhinology 64: 5, 0 - 0, 2026
https://doi.org/10.4193/Rhin25.558

Received for publication:
October 1 , 2025
Accepted: May 26, 2026

Associate Editor:
Michael Soyka

This manuscript contains online supplementary material

SUPPLEMENTARY MATERIAL

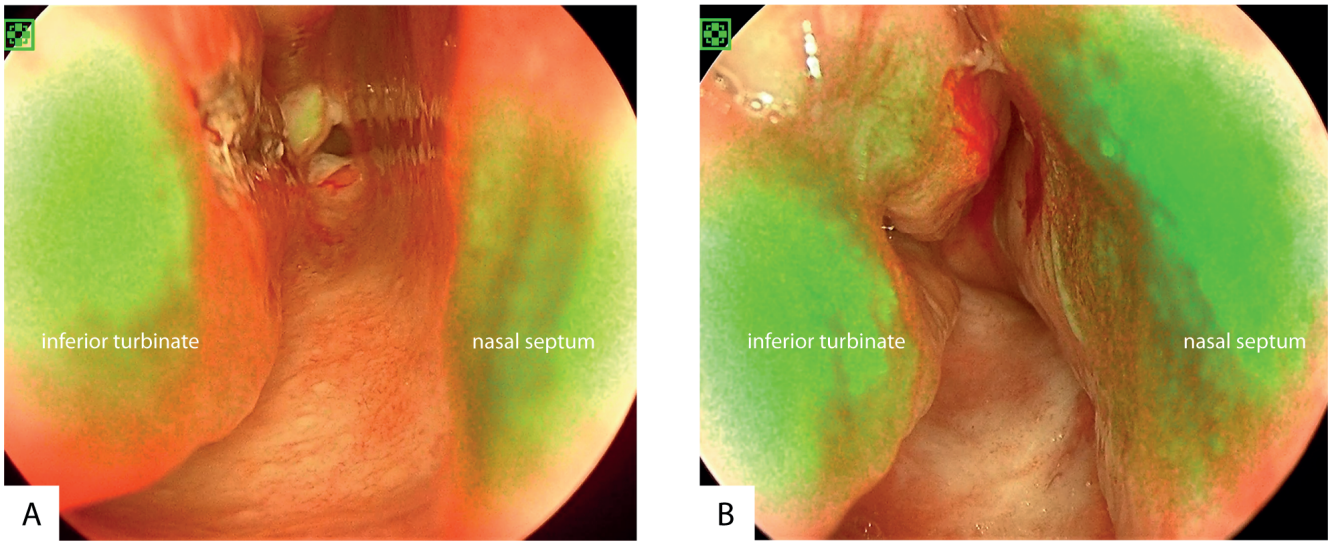

Figure S1. Delayed excretion of ICG in the nasal septum and inferior turbinate. (A)(B) Intraoperatively, fluorescence was observed in the nasal septum and inferior turbinate, whereas no fluorescence was detected in the nasal floor.

Table S1. ICG injection patterns and ICG Fluorescence Imaging Effects in 46 Cases of rNPC.

Case	Injection time	Preoperative injection dose (mg/kg)	Intraopera-tive dosage per injection mg	Tumour imaging before intraop-erative injection (ICG_pre)a	Tumour imaging after intraop-erative injection (ICG_post)a	ICG localization
1	intraoperative		2.5		moderate	yes
2	intraoperative		2.5		strong	yes
3	intraoperative		2.5		strong	yes
4	intraoperative		2.5		strong	yes
5	preoperative 3h	0.5	2.5	non-fluorescent	weak	yes
6	preoperative 3h	0.5	2.5	non-fluorescent	strong	yes
7	preoperative 3h	0.5	2.5	moderate	strong	yes
8	preoperative 3h	0.5	2.5	non-fluorescent	strong	yes
9	preoperative 3h	0.5	2.5	weak	strong	yes
10	preoperative 3h	0.5	2.5	non-fluorescent	strong	yes
11	preoperative 6h	0.5	2.5	strong	strong	yes
12	preoperative 6h	0.5	2.5	strong	strong	yes
13	preoperative 6h	0.5	2.5	non-fluorescent	strong	yes
14	preoperative 6h	0.5	2.5	non-fluorescent	non-fluorescent	no
15	preoperative 6h	0.5	2.5	strong	strong	yes
16	preoperative 12h	0.5	2.5	moderate	strong	yes
17	preoperative 12h	0.5	2.5	weak	weak	no
18	preoperative 12h	0.5	2.5	strong	strong	yes
19	preoperative 12h	0.5	2.5	moderate	moderate	yes
20	preoperative 3h	0.6	2.5	strong	strong	yes

Case	Injection time	Preoperative injection dose (mg/kg)	Intraoperative dosage per injection mg	Tumour imaging before intraoperative injection (ICG_pre)a	Tumour imaging after intraoperative injection (ICG_post)a	ICG localization
21	preoperative 3h	0.6	2.5	non-fluorescent	strong	yes
22	preoperative 3h	0.6	2.5	non-fluorescent	strong	yes
23	preoperative 3h	0.6	2.5	non-fluorescent	non-fluorescent	no
24	preoperative 3h	0.6	2.5	strong	strong	yes
25	preoperative 3h	0.6	2.5	strong	strong	yes
26	preoperative 6h	0.6	2.5	strong	strong	yes
27	preoperative 6h	0.6	2.5	non-fluorescent	moderate	yes
28	preoperative 6h	0.6	2.5	non-fluorescent	non-fluorescent	no
29	preoperative 6h	0.6	2.5	strong	strong	yes
30	preoperative 6h	0.6	2.5	strong	strong	yes
31	preoperative 6h	0.6	2.5	strong	strong	yes
32	preoperative 12h	0.6	2.5	weak	strong	yes
33	preoperative 12h	0.6	2.5	weak	moderate	yes
34	preoperative 12h	0.6	2.5	strong	strong	yes
35	preoperative 12h	0.6	2.5	strong	strong	yes
36	preoperative 3h	0.7	2.5	weak	strong	yes
37	preoperative 3h	0.7	2.5	non-fluorescent	non-fluorescent	no
38	preoperative 3h	0.7	2.5	moderate	strong	yes
39	preoperative 6h	0.7	2.5	weak	strong	yes
40	preoperative 6h	0.7	2.5	strong	strong	yes
41	preoperative 6h	0.7	2.5	moderate	strong	yes
42	preoperative 6h	0.7	2.5	strong	strong	yes
43	preoperative 6h	0.7	2.5	moderate	strong	yes
44	preoperative 12h	0.7	2.5	weak	strong	yes
45	preoperative 12h	0.7	2.5	weak	strong	yes
46	preoperative 12h	0.7	2.5	strong	strong	yes

ICG fluorescence imaging efficacy: if the fluorescence intensity in the target area is greater than that of the inferior turbinate, the fluorescence imaging effect is considered strong. If the fluorescence intensity in the target area is comparable to that of the inferior turbinate, the fluorescence imaging effect is considered moderate. If the fluorescence intensity in the target area is less than that of the inferior turbinate, the fluorescence imaging effect is considered weak.

Table S2. The intravenous injection dose and timing of ICG and ICG fluorescence imaging effects in 36 cases of non-tumour.

Case	Injection time	Preoperative injection dose (mg/kg)	Intraoperative dosage per injection mg	Tumour imaging before intraoperative injection (ICG_pre)a	Tumour imaging after intraoperative injection (ICG_post)a	ICG localization
1	intraoperative				non-fluorescent	no
2	preoperative 3h	0.5	2.5	non-fluorescent	non-fluorescent	no
3	preoperative 3h	0.5	2.5	non-fluorescent	non-fluorescent	no
4	preoperative 3h	0.5	2.5	non-fluorescent	non-fluorescent	no
5	preoperative 3h	0.5	2.5	non-fluorescent	non-fluorescent	no
6	preoperative 3h	0.5	2.5	non-fluorescent	non-fluorescent	no
7	preoperative 3h	0.5	2.5	non-fluorescent	non-fluorescent	no
8	preoperative 6h	0.5	2.5	non-fluorescent	moderate	yes
9	preoperative 12h	0.5	2.5	non-fluorescent	moderate	yes
10	preoperative 12h	0.5	2.5	non-fluorescent	non-fluorescent	no
11	preoperative 3h	0.6	2.5	non-fluorescent	non-fluorescent	no
12	preoperative 3h	0.6	2.5	non-fluorescent	weak	yes
13	preoperative 3h	0.6	2.5	non-fluorescent	non-fluorescent	no
14	preoperative 3h	0.6	2.5	non-fluorescent	weak	yes
15	preoperative 3h	0.6	2.5	non-fluorescent	non-fluorescent	no
16	preoperative 3h	0.6	2.5	non-fluorescent	non-fluorescent	no
17	preoperative 3h	0.6	2.5	non-fluorescent	non-fluorescent	no
18	preoperative 6h	0.6	2.5	weak	weak	yes
19	preoperative 6h	0.6	2.5	non-fluorescent	non-fluorescent	no
20	preoperative 6h	0.6	2.5	non-fluorescent	non-fluorescent	no
21	preoperative 6h	0.6	2.5	weak	weak	yes
22	preoperative 6h	0.6	2.5	non-fluorescent	non-fluorescent	no
23	preoperative 12h	0.6	2.5	non-fluorescent	weak	yes
24	preoperative 12h	0.6	2.5	non-fluorescent	non-fluorescent	no
25	preoperative 12h	0.6	2.5	non-fluorescent	non-fluorescent	no
26	preoperative 3h	0.7	2.5	non-fluorescent	non-fluorescent	no
27	preoperative 3h	0.7	2.5	non-fluorescent	weak	yes
28	preoperative 6h	0.7	2.5	non-fluorescent	weak	no
29	preoperative 12h	0.7	2.5	non-fluorescent	non-fluorescent	no
30	preoperative 12h	0.7	2.5	non-fluorescent	non-fluorescent	no
31	preoperative 12h	0.7	2.5	non-fluorescent	non-fluorescent	no
32	preoperative 12h	0.7	2.5	non-fluorescent	non-fluorescent	no
33	preoperative 12h	0.6	2.5	non-fluorescent	non-fluorescent	no
34	preoperative 12h	0.5	2.5	non-fluorescent	weak	yes
35	preoperative 3h	0.7	2.5	non-fluorescent	non-fluorescent	no
36	preoperative 6h	0.6	2.5	weak	moderate	yes

Additional file. The original ICG fluorescence images of other rNPC patients.

Case 1

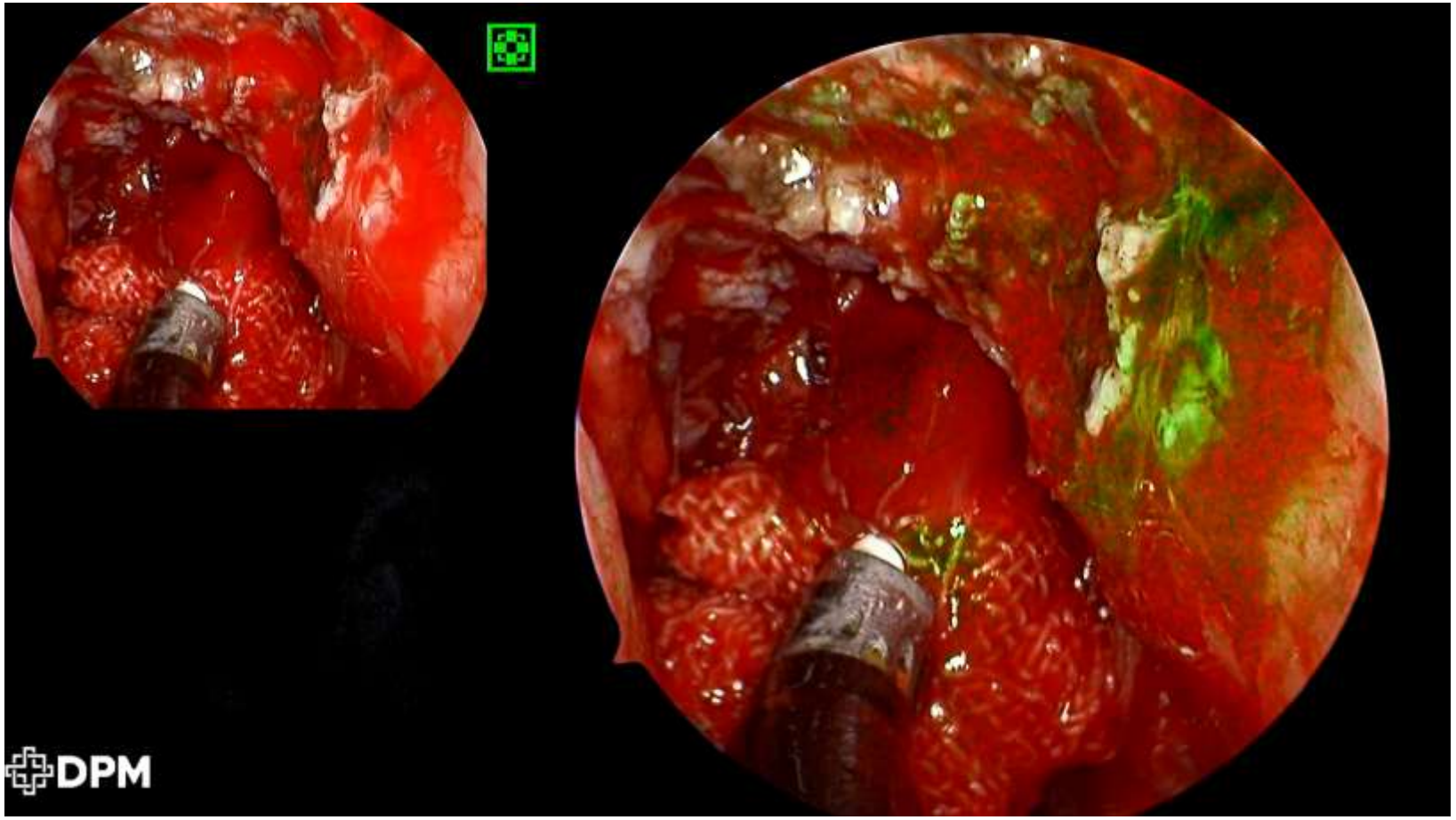

Case 2

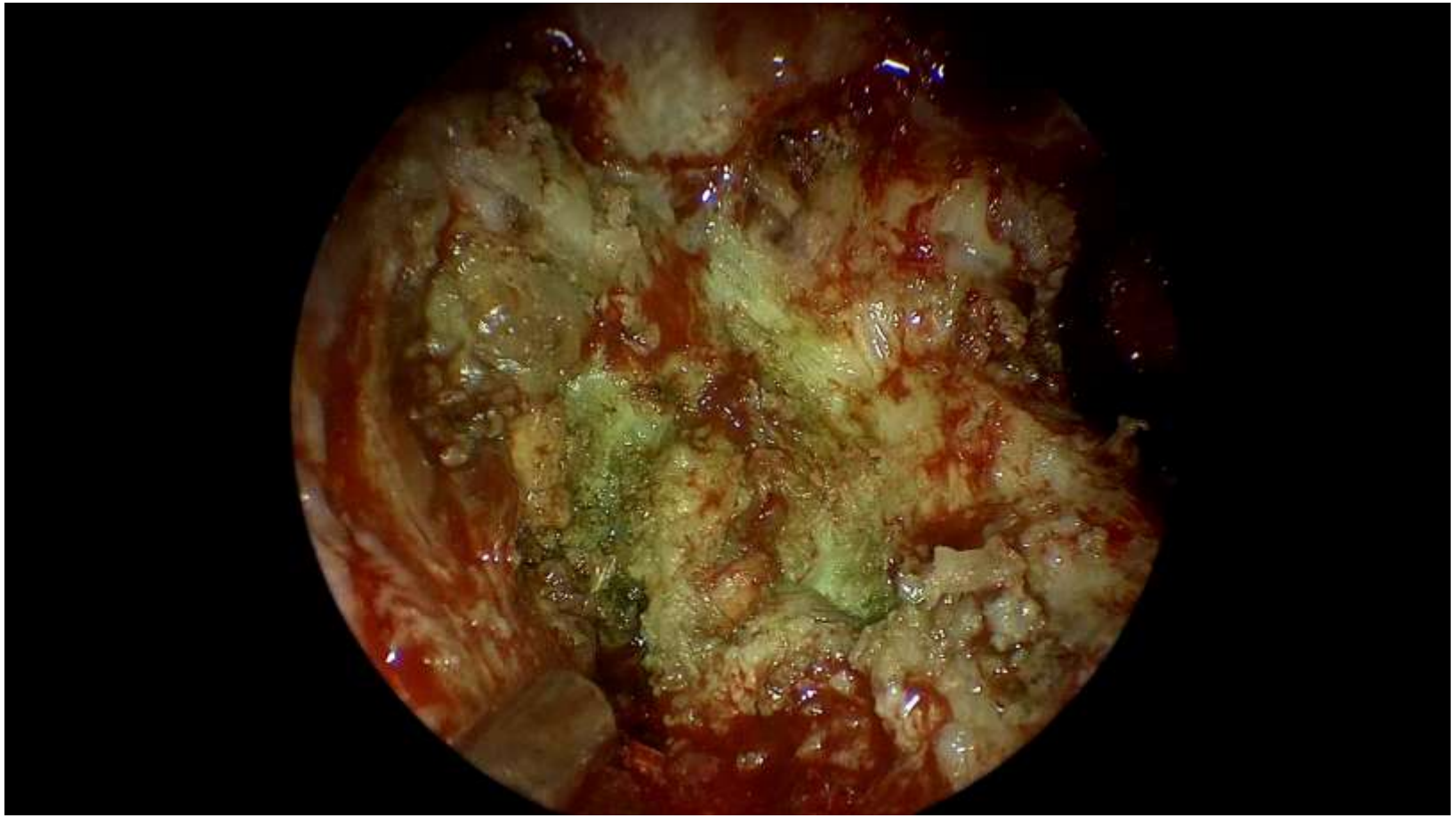

Case 3

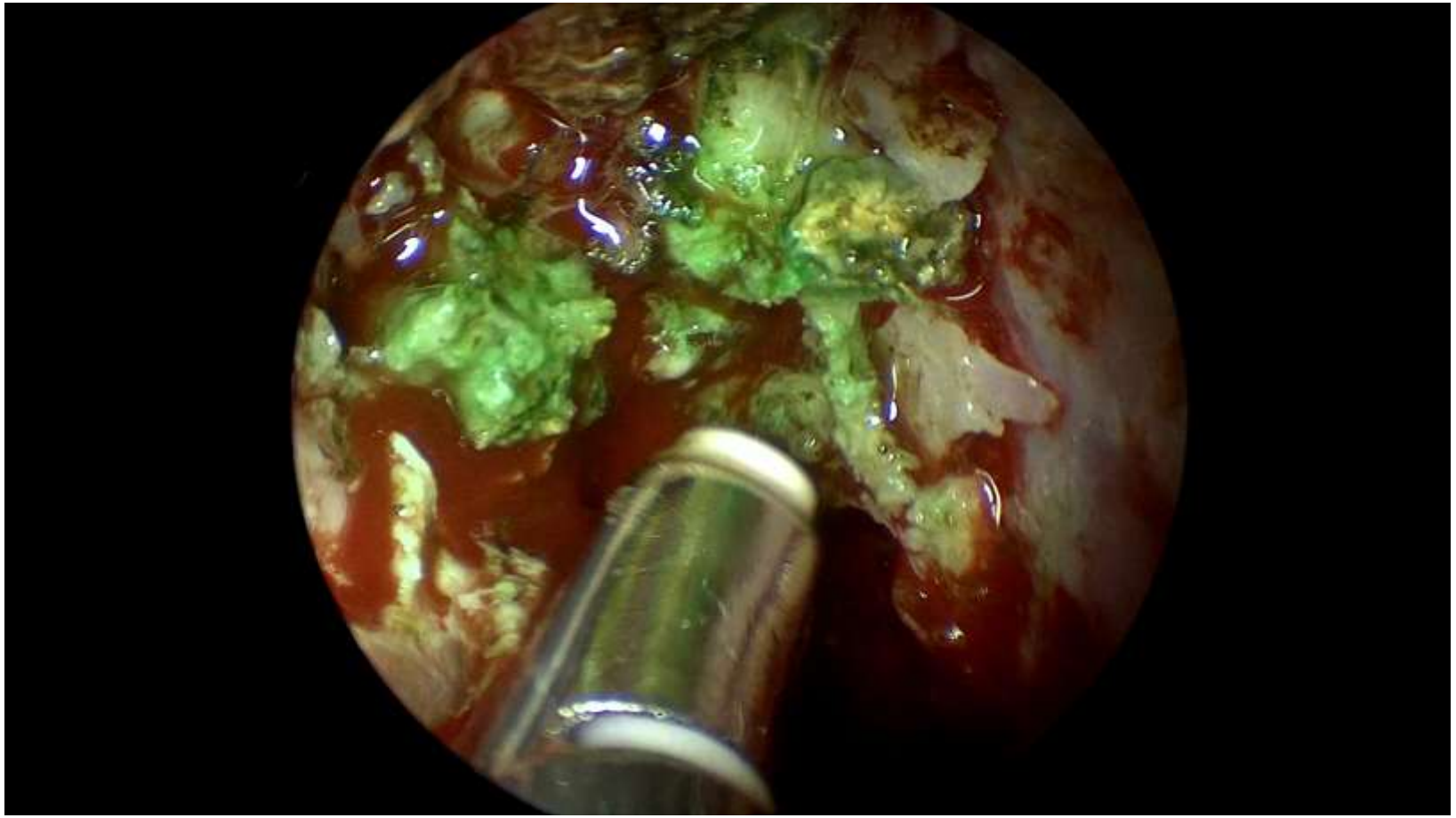

Case 4

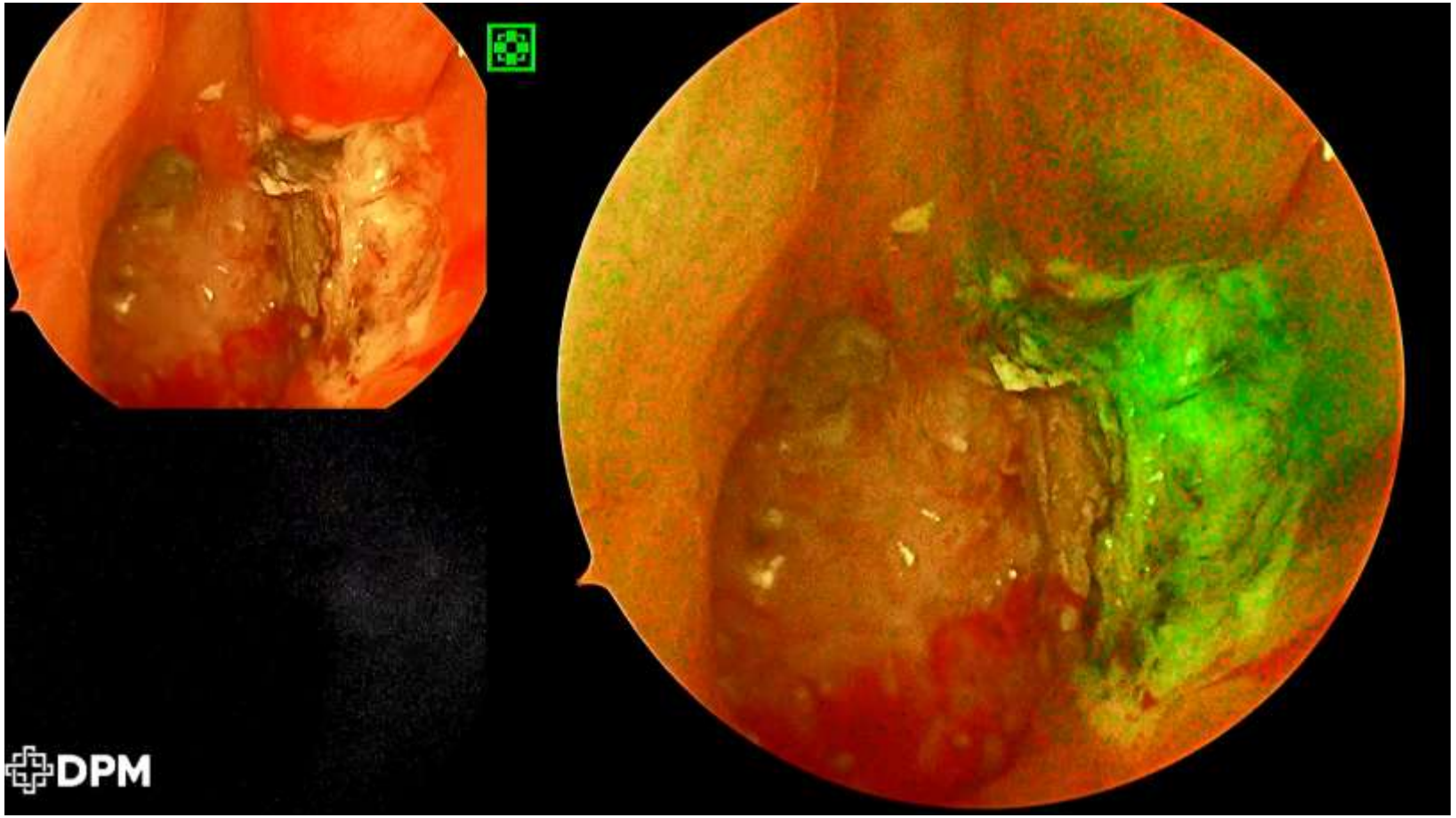

Case 5

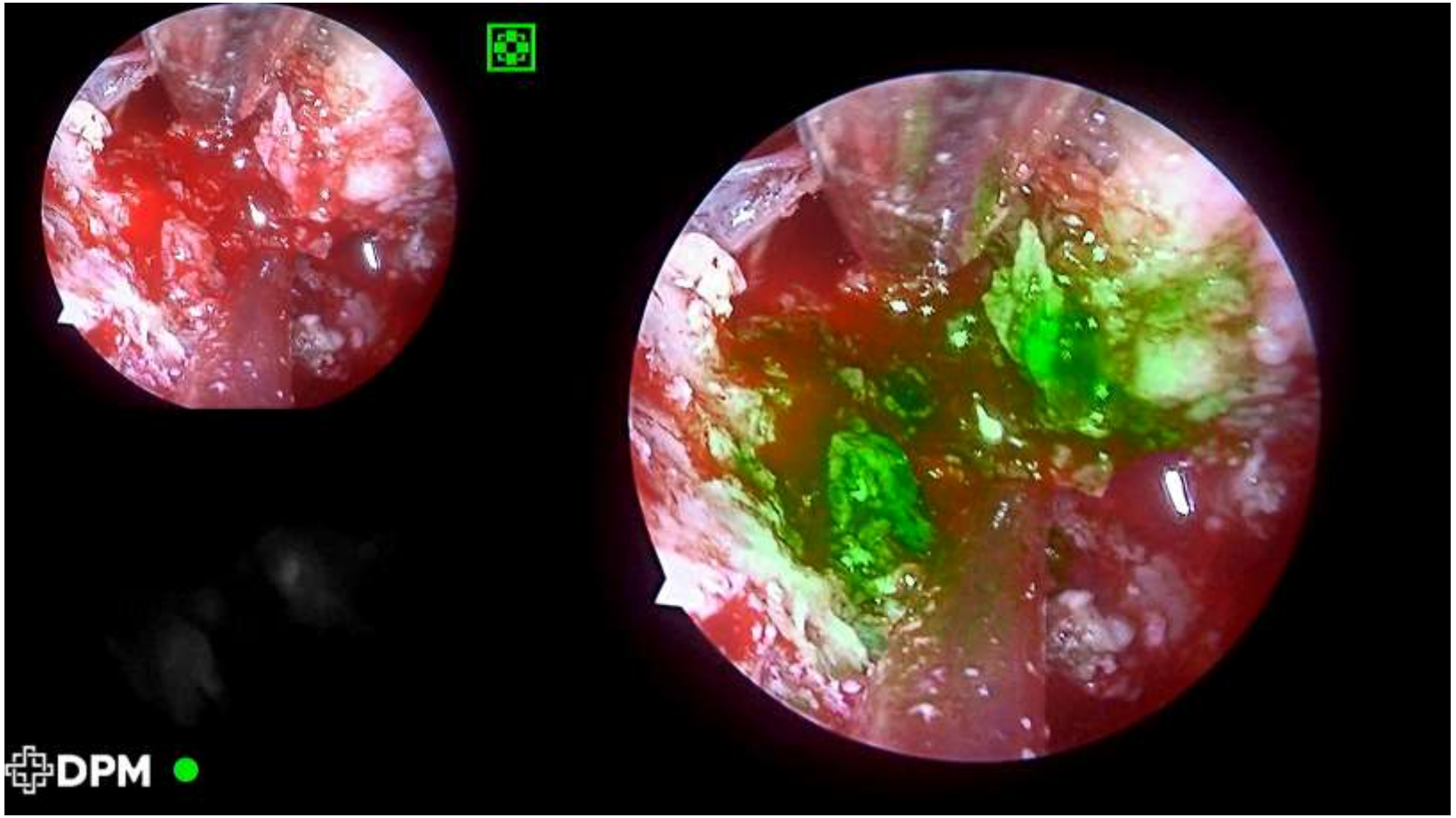

Case 6

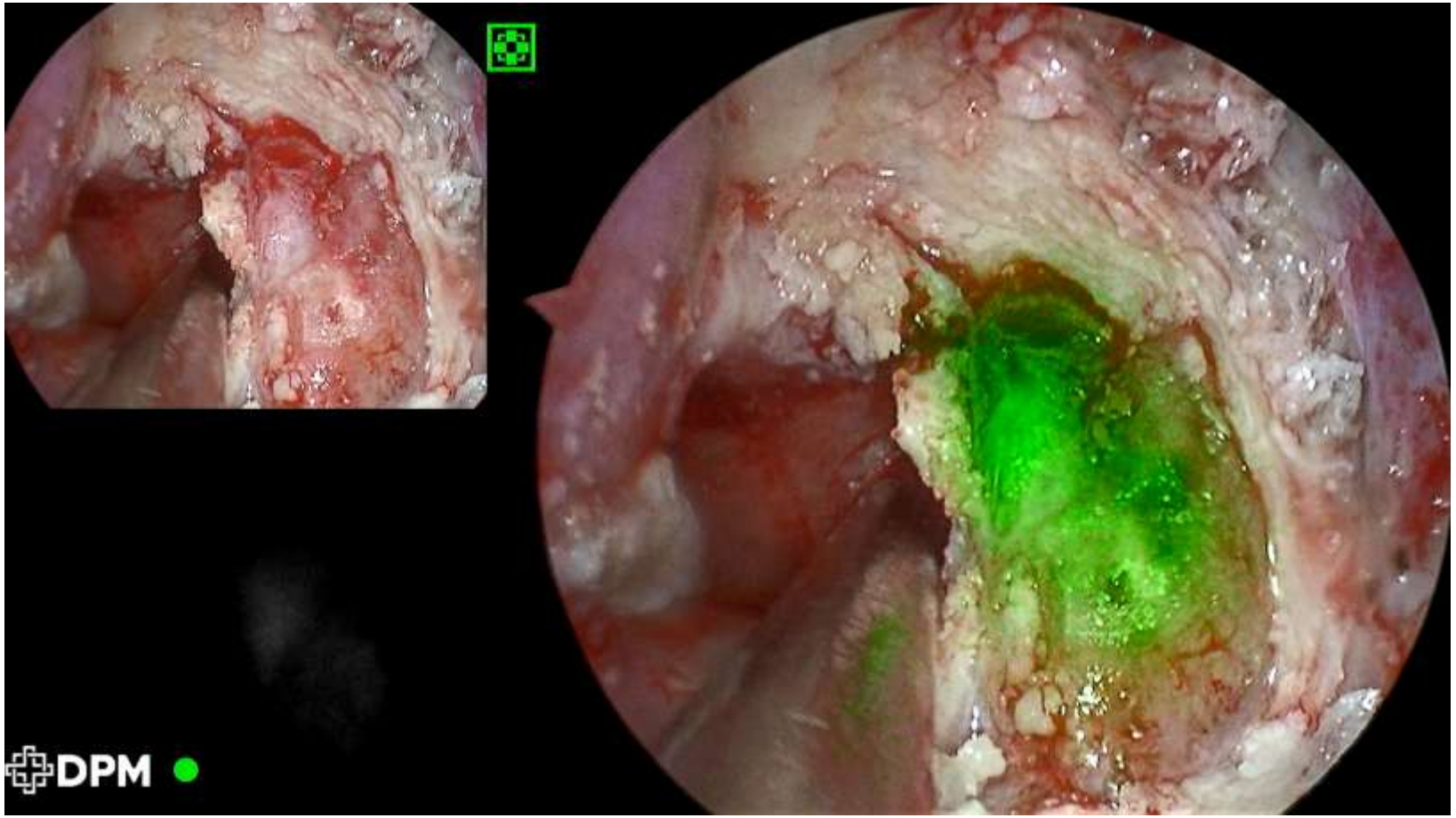

Case 8

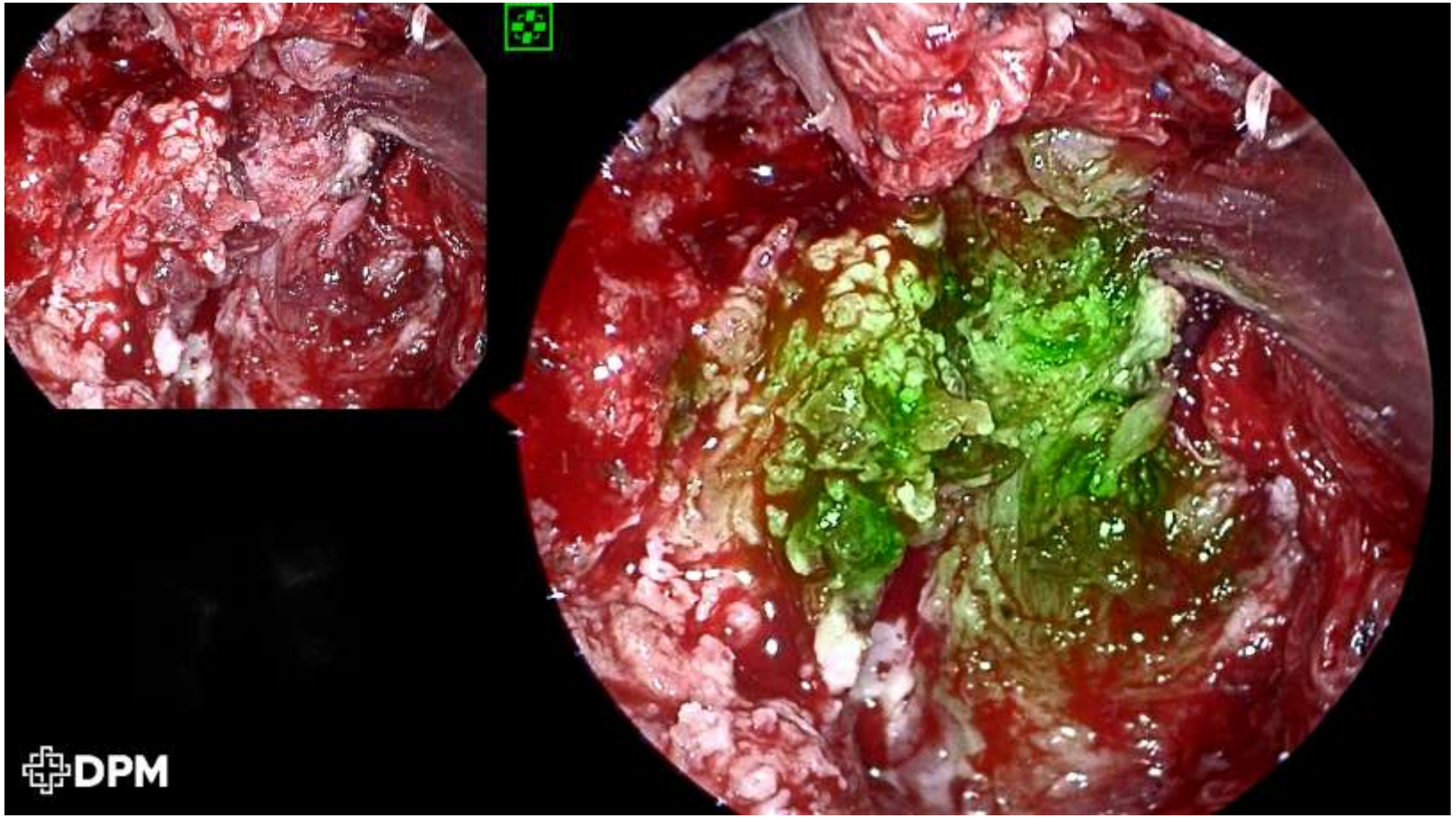

Case 9

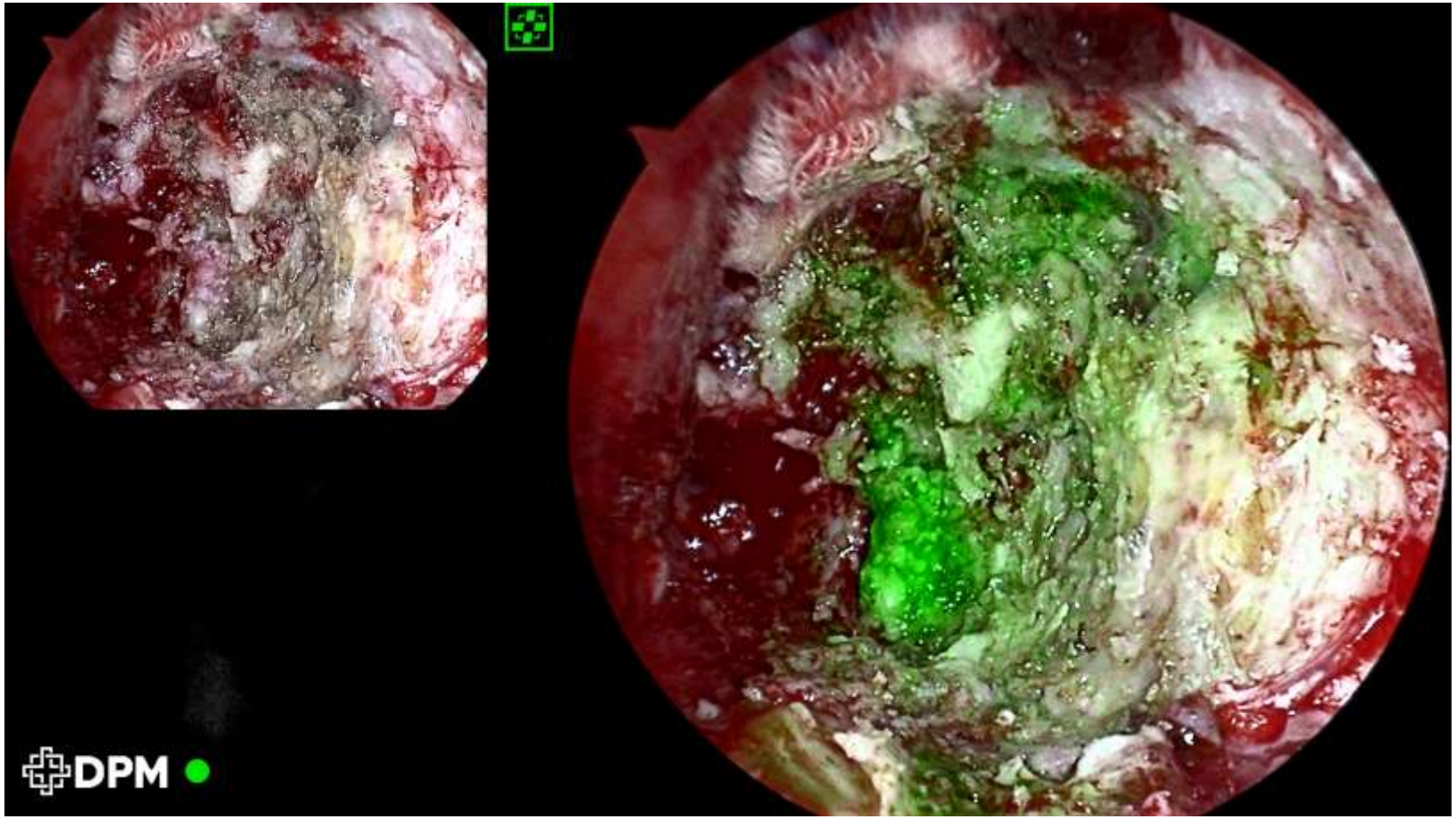

Case 10

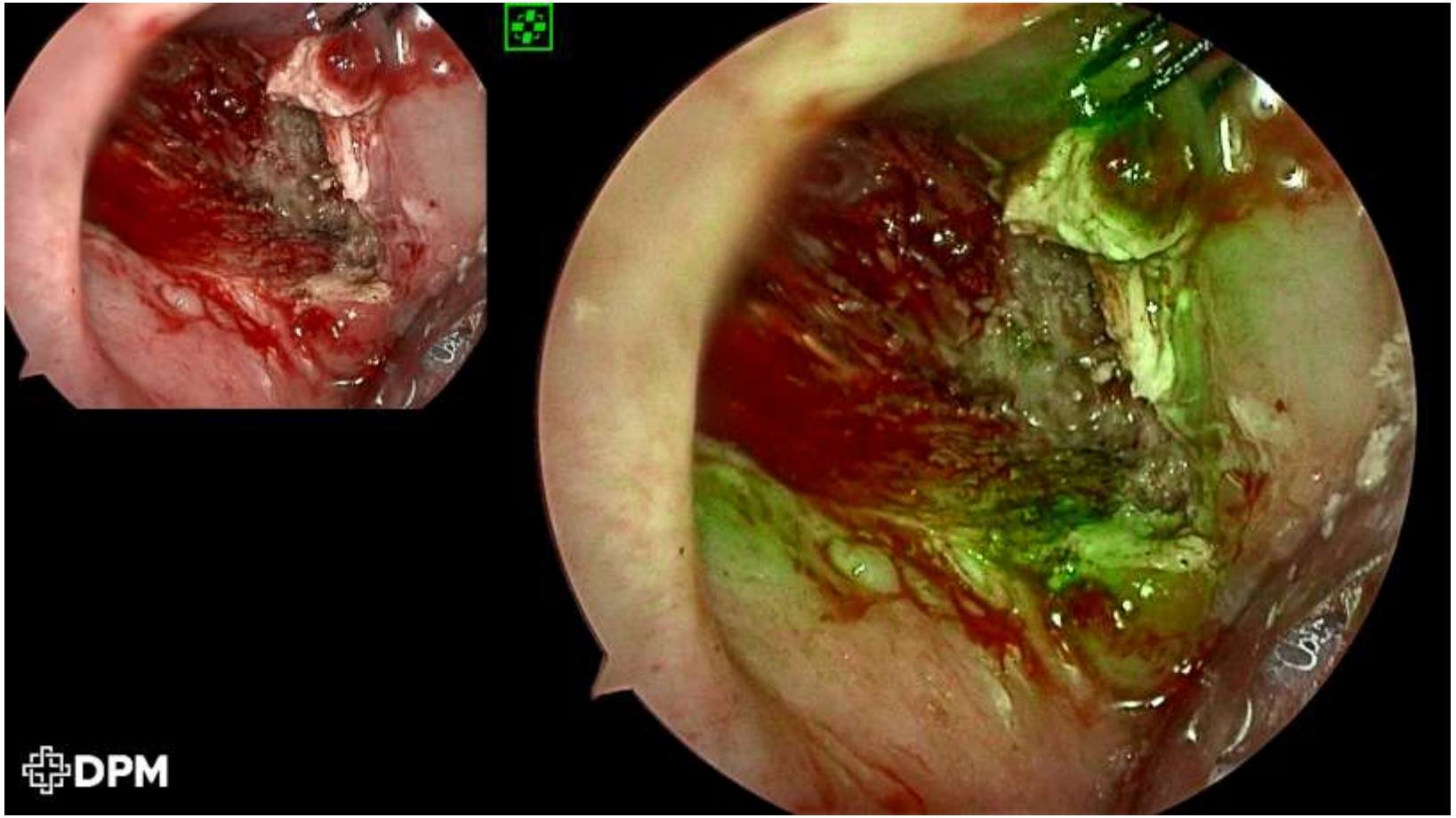

Case 11

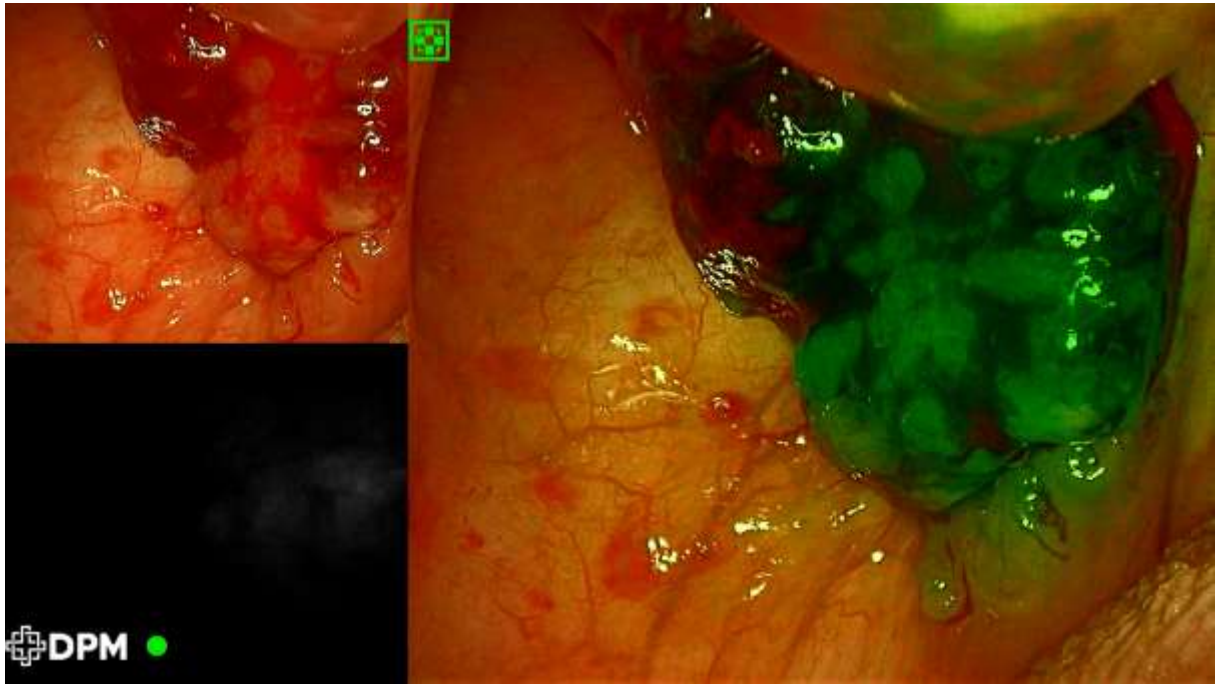

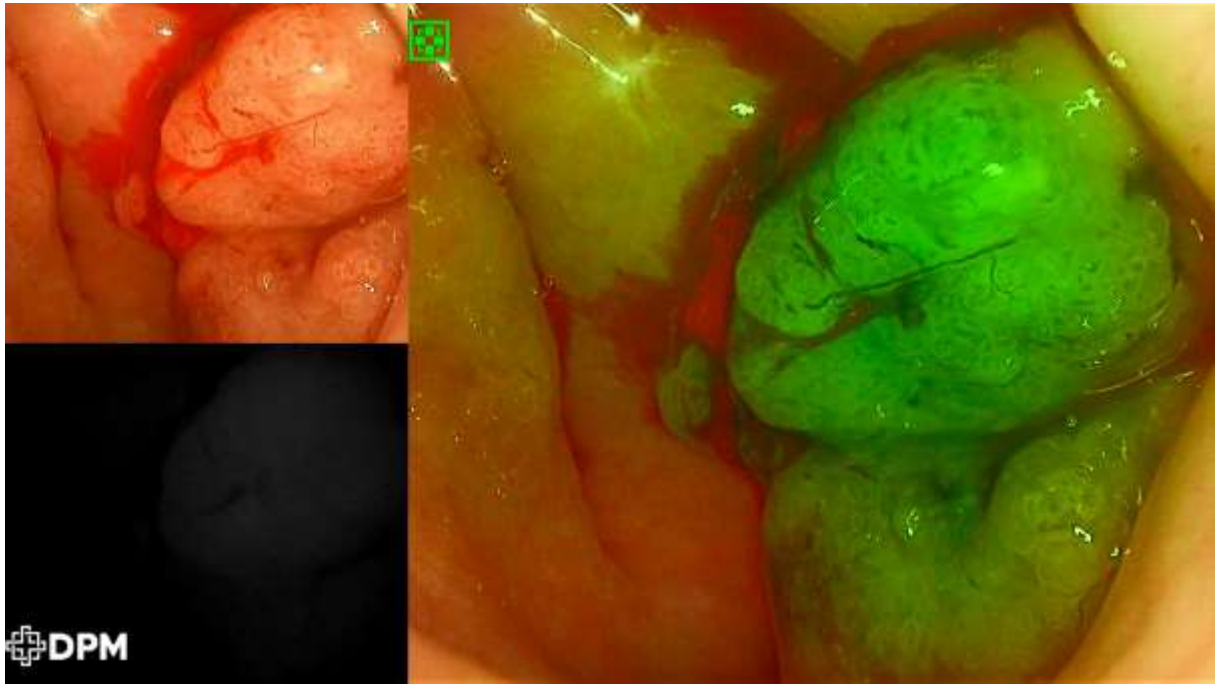

Case 12

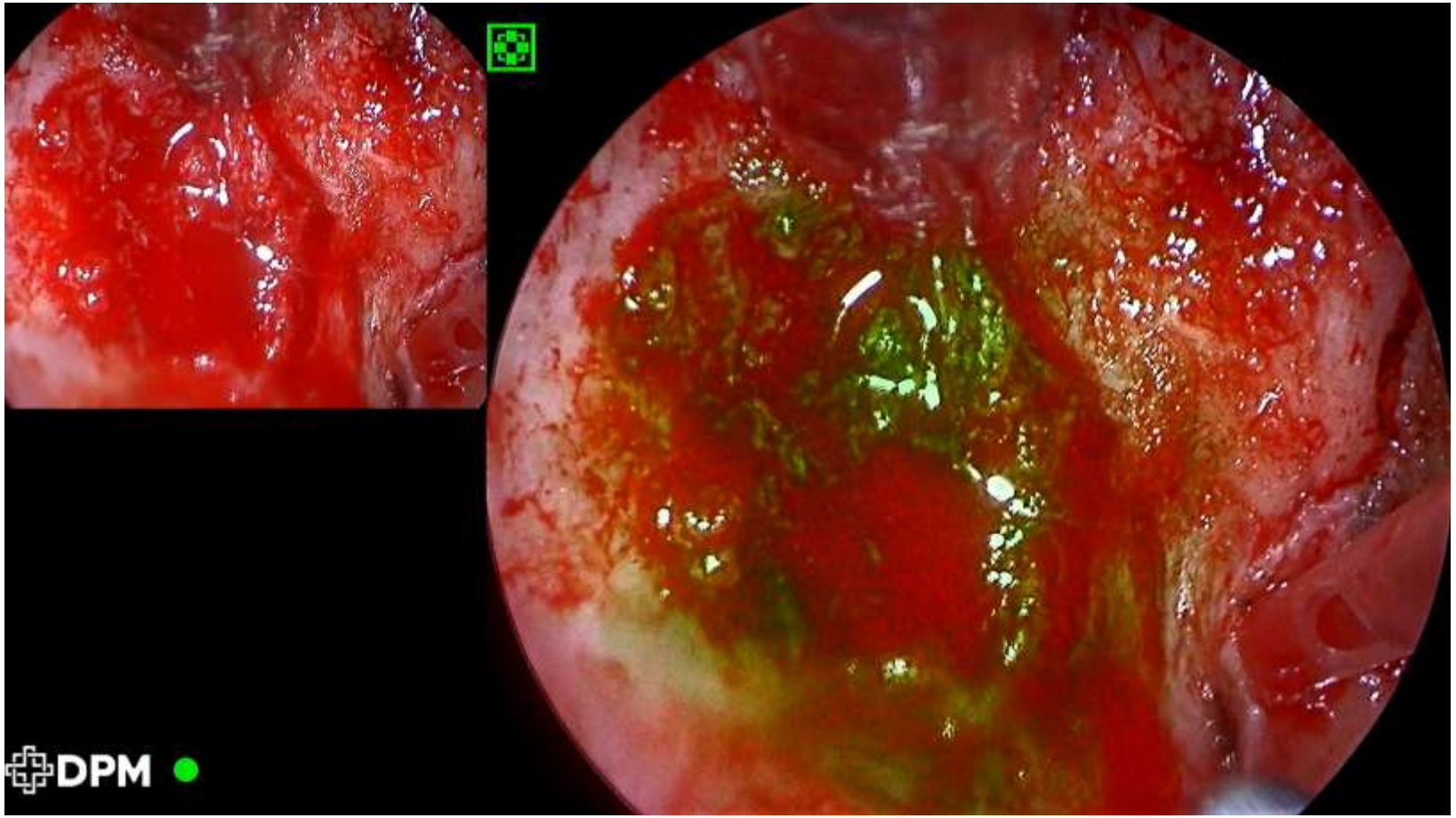

Case 13

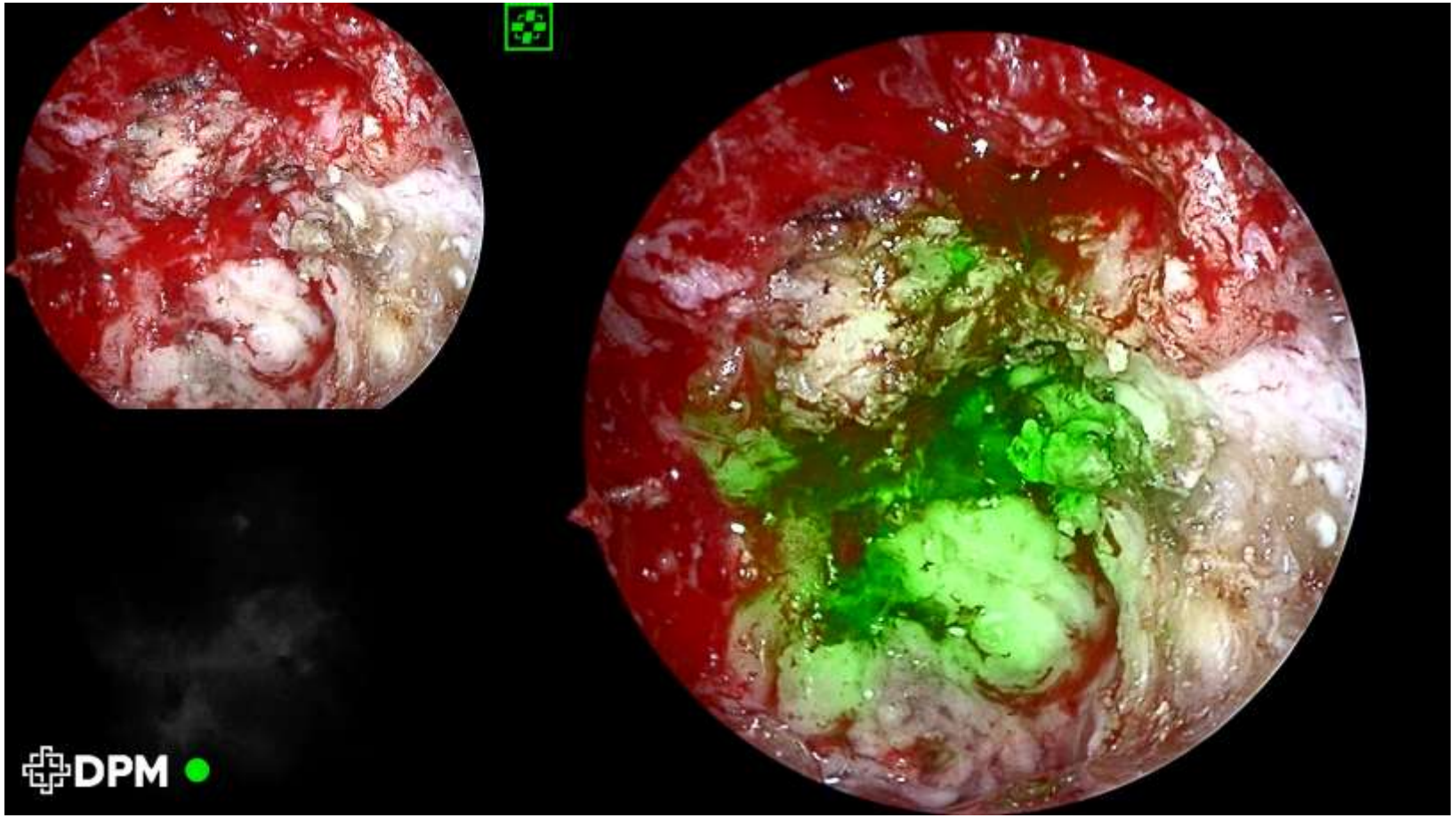

Case 15

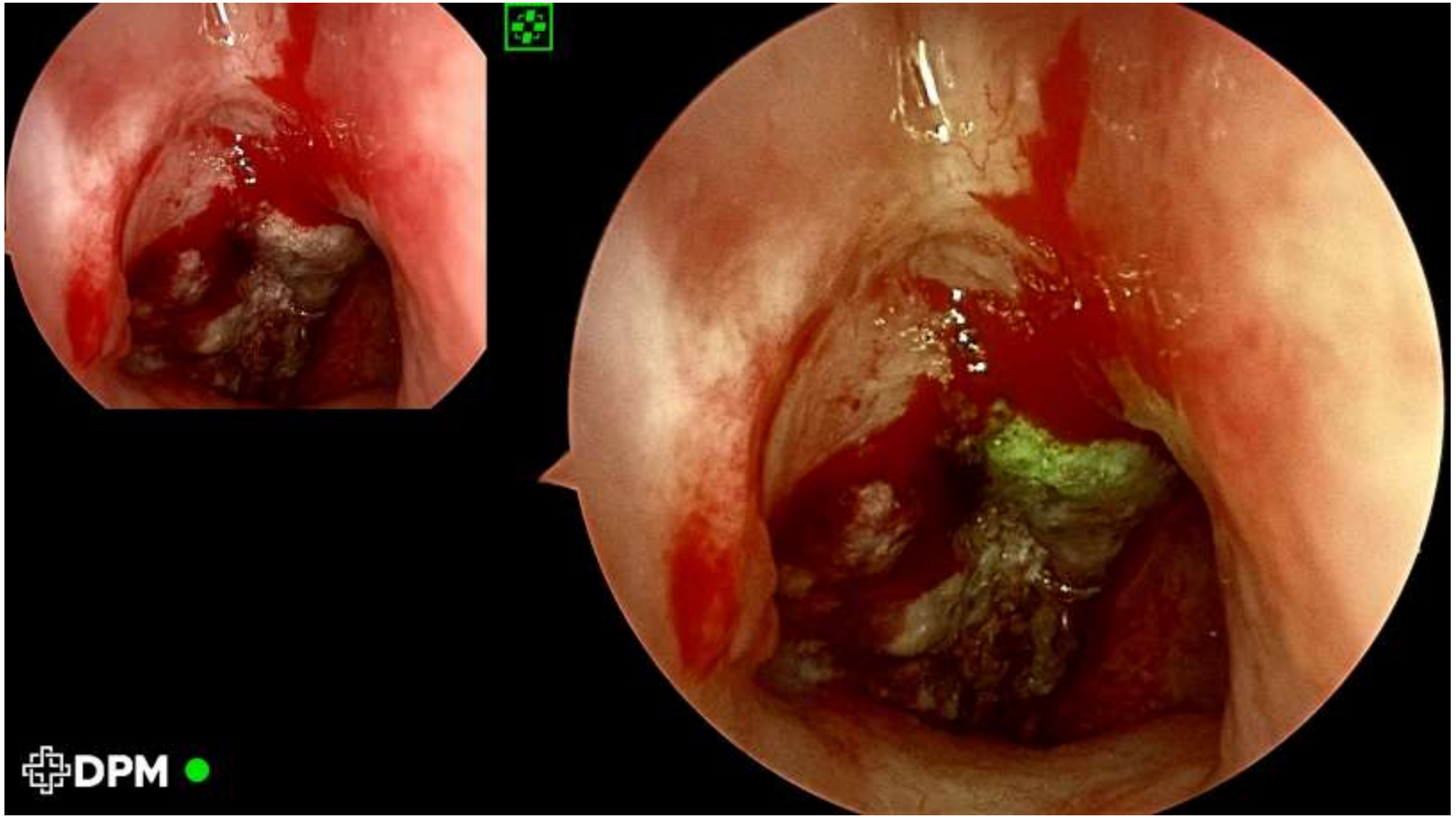

Case 16

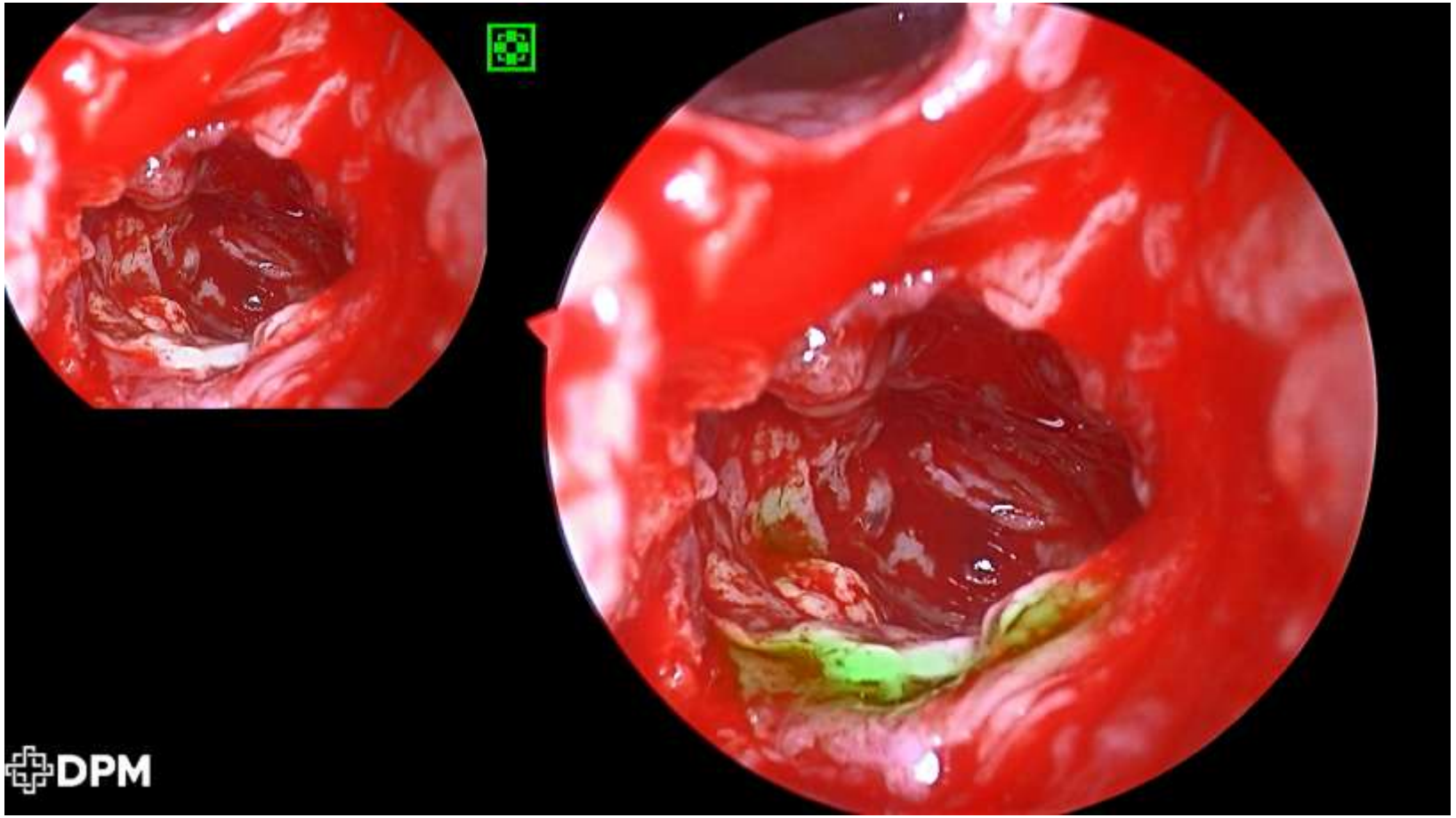

Case 19

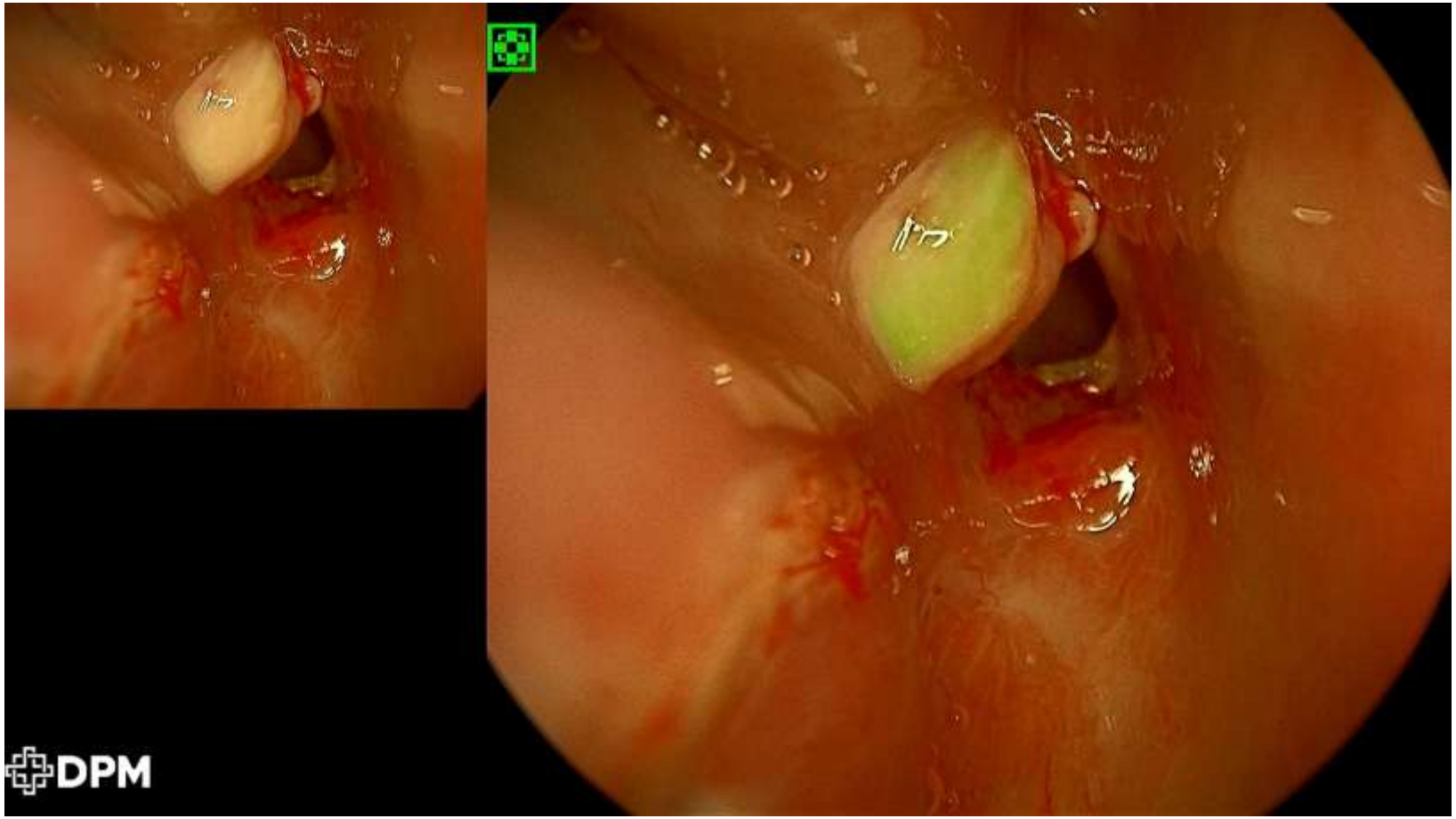

Case 20

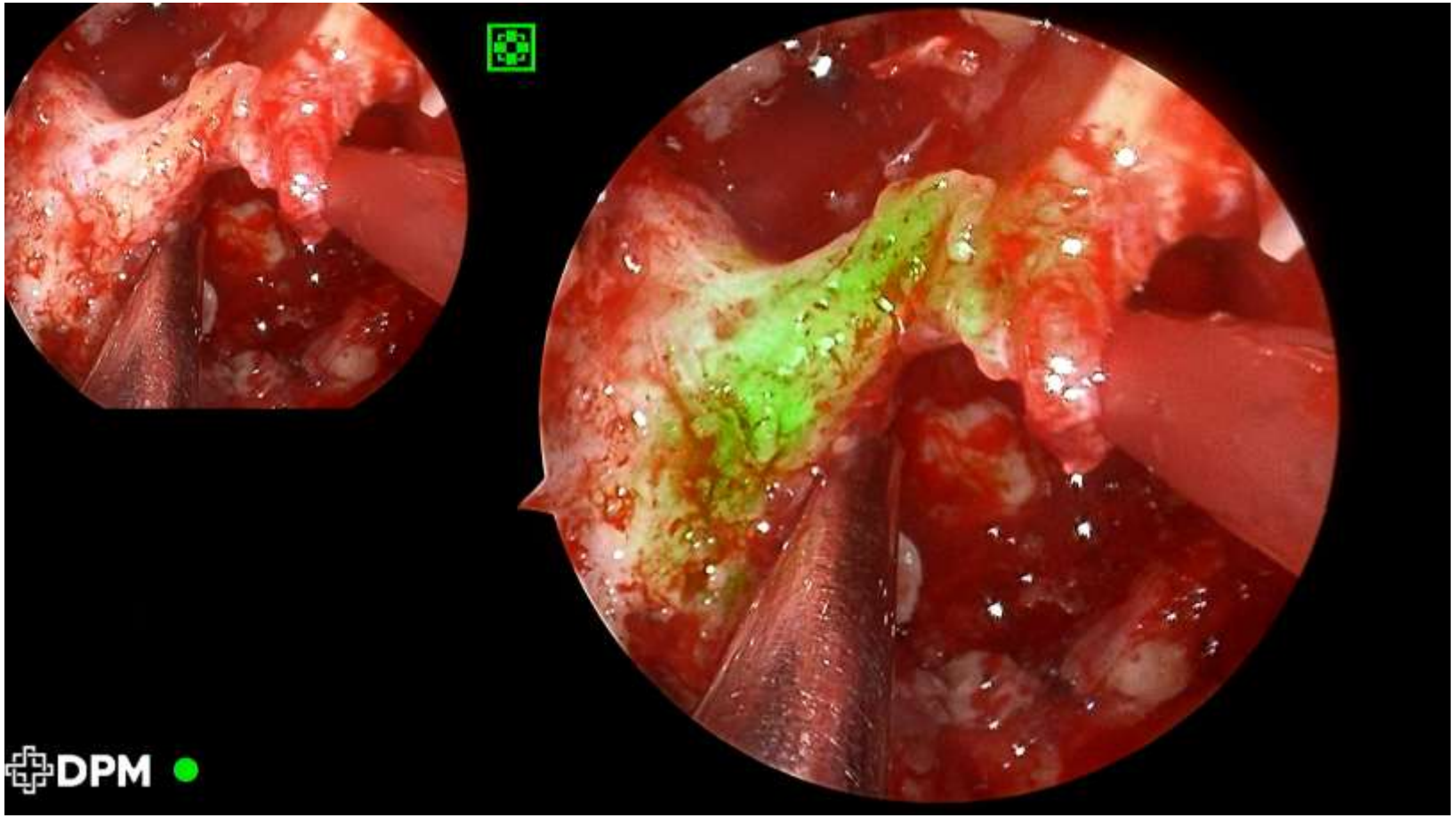

Case 21

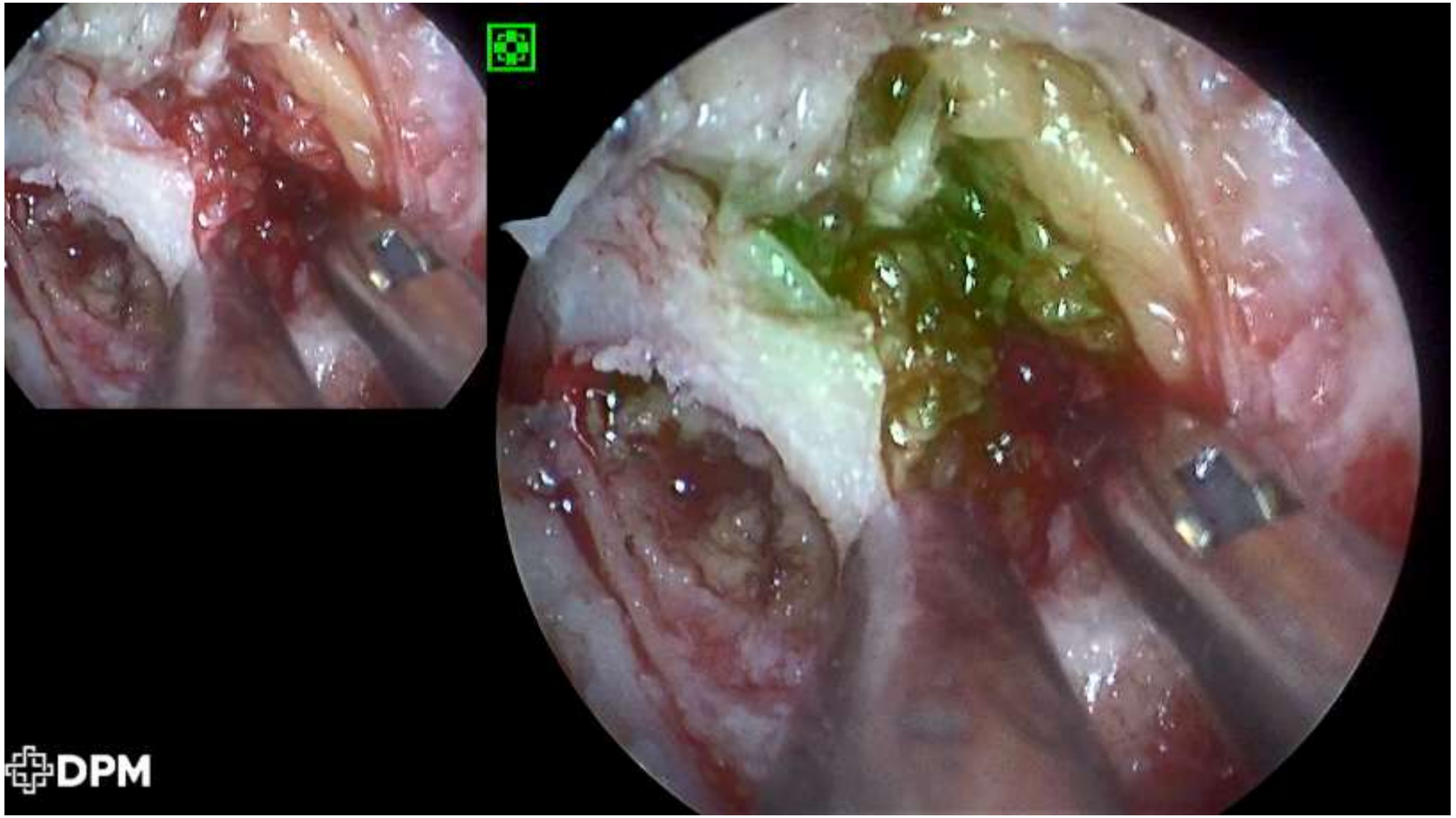

Case 22

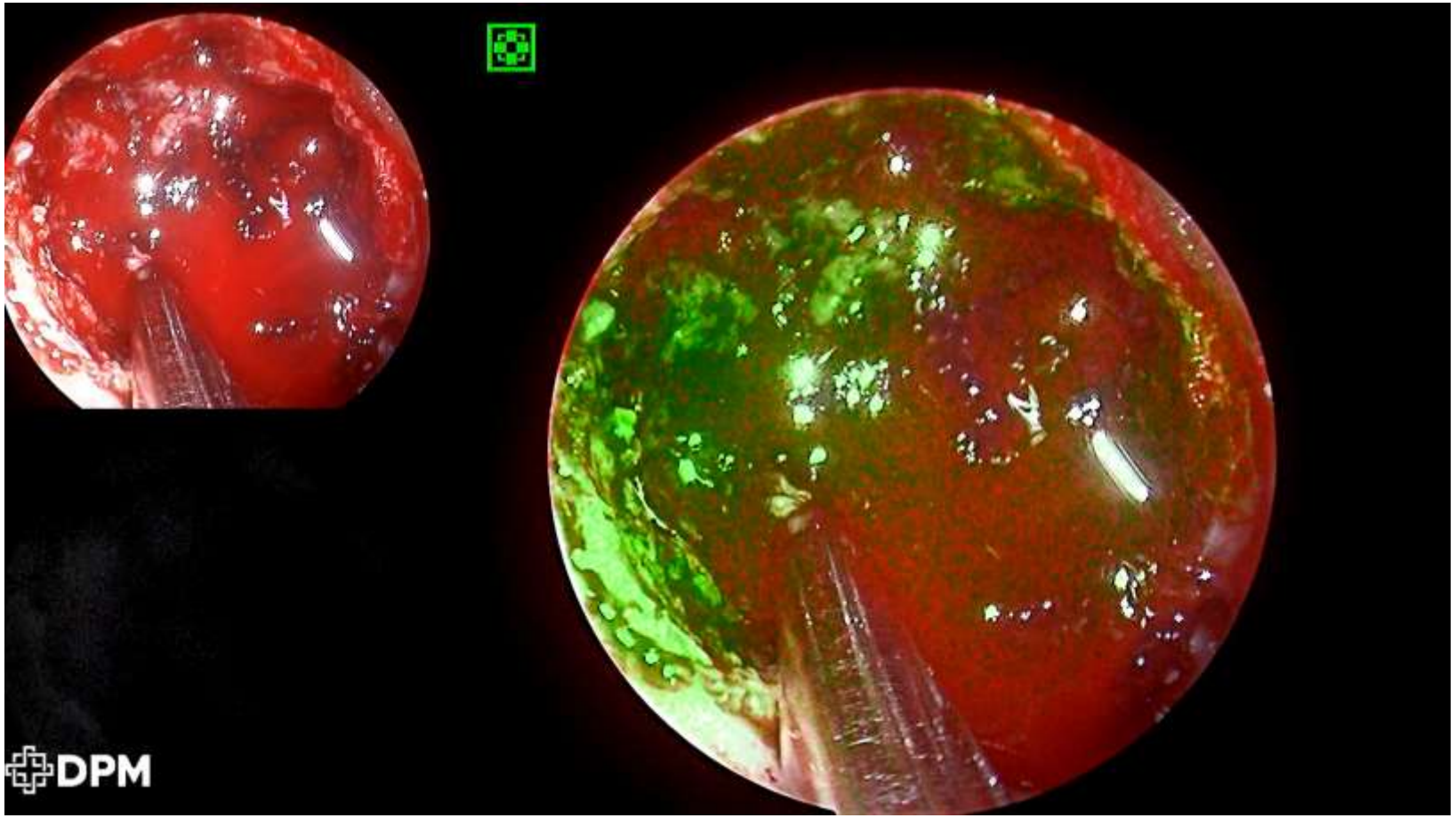

Case 24

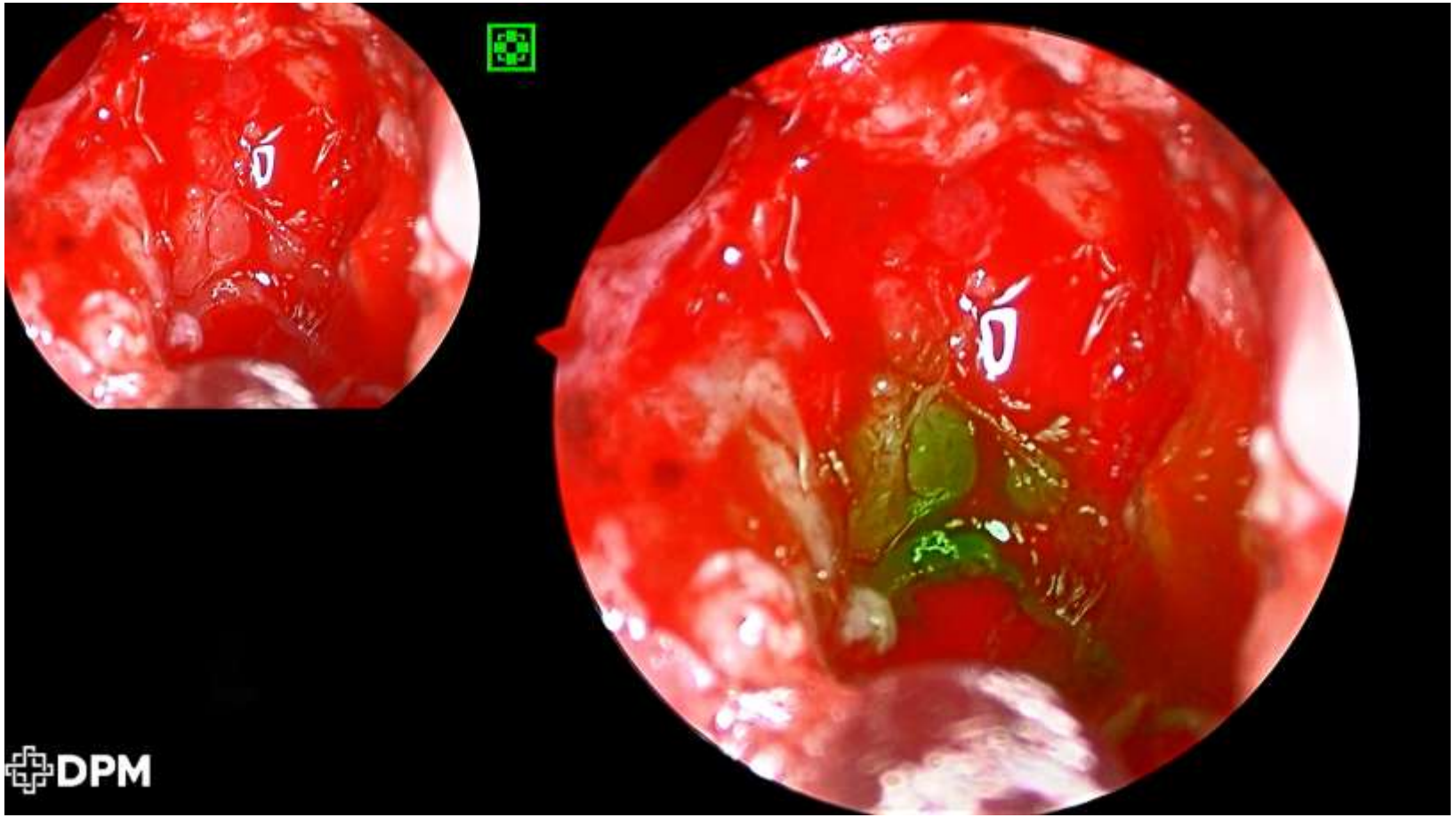

Case 25

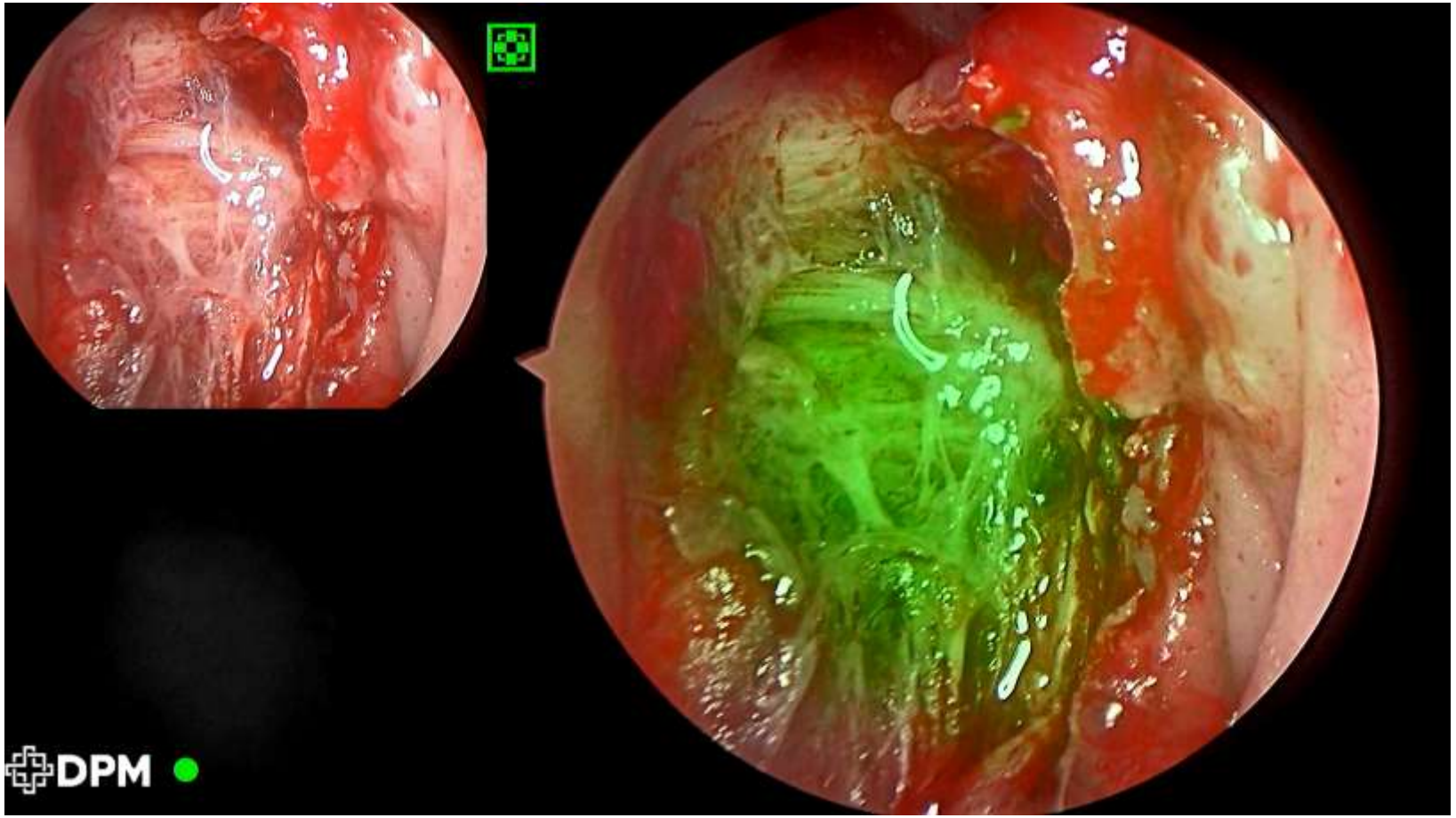

Case 26

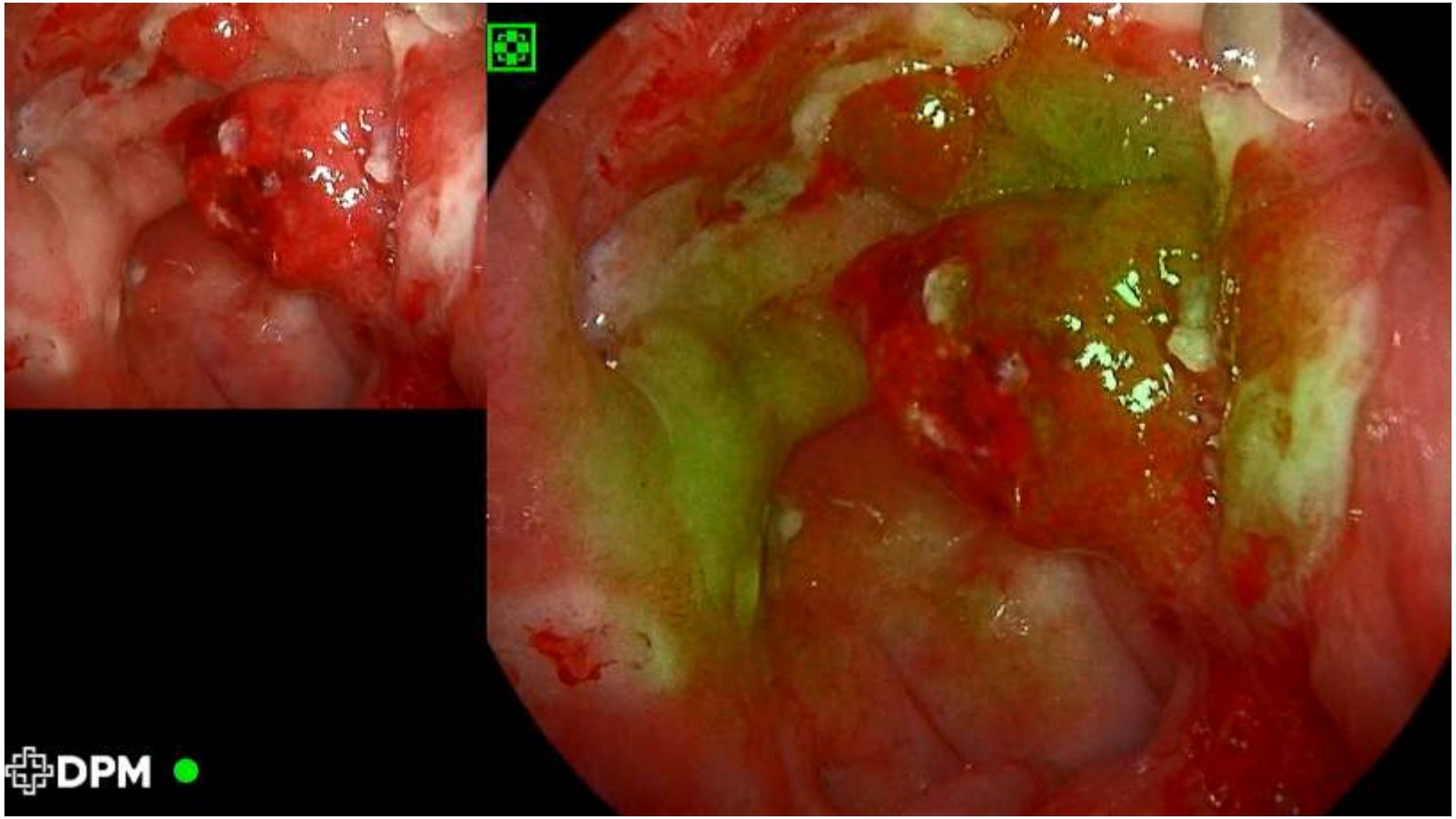

Case 27

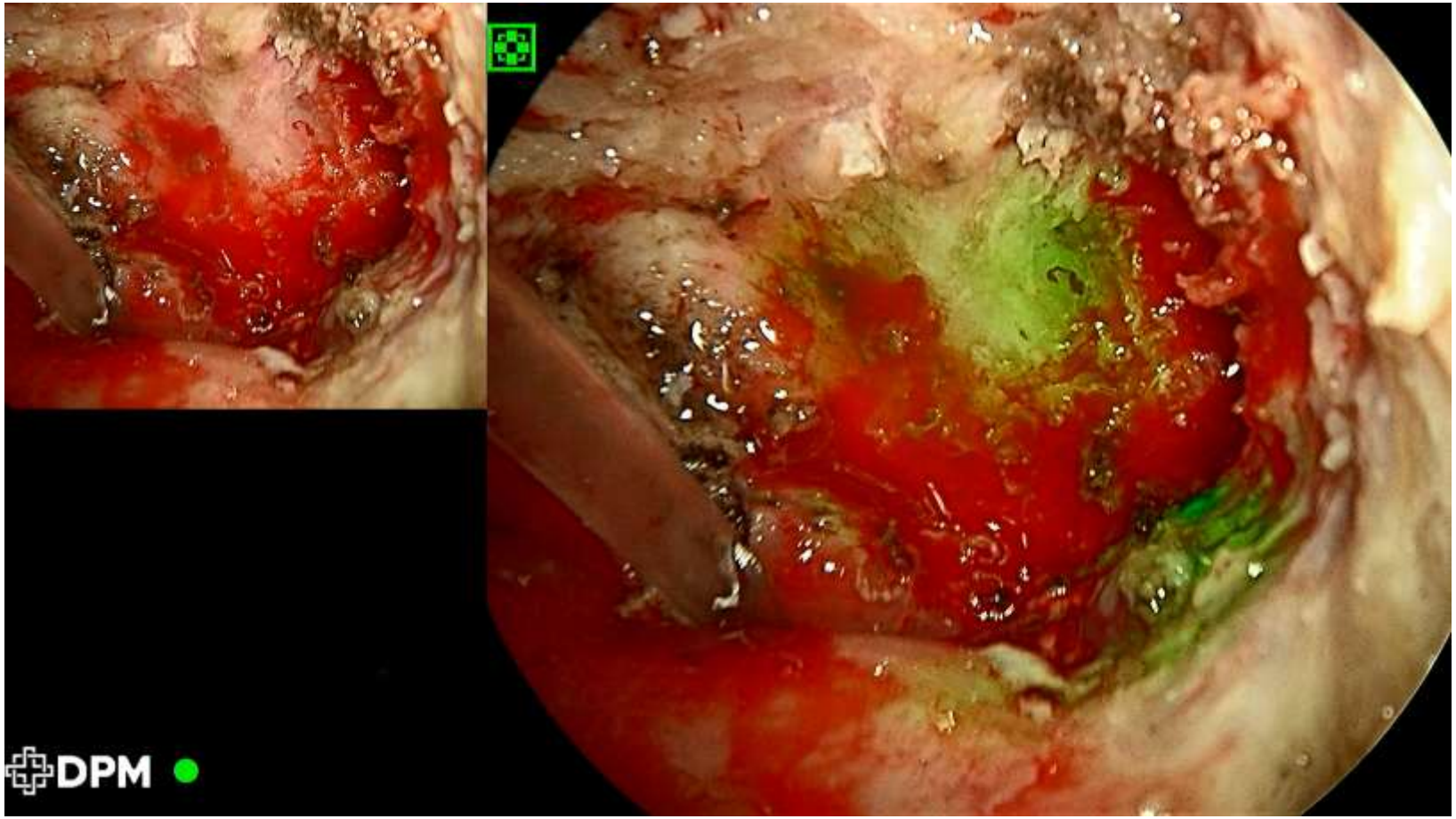

Case 29

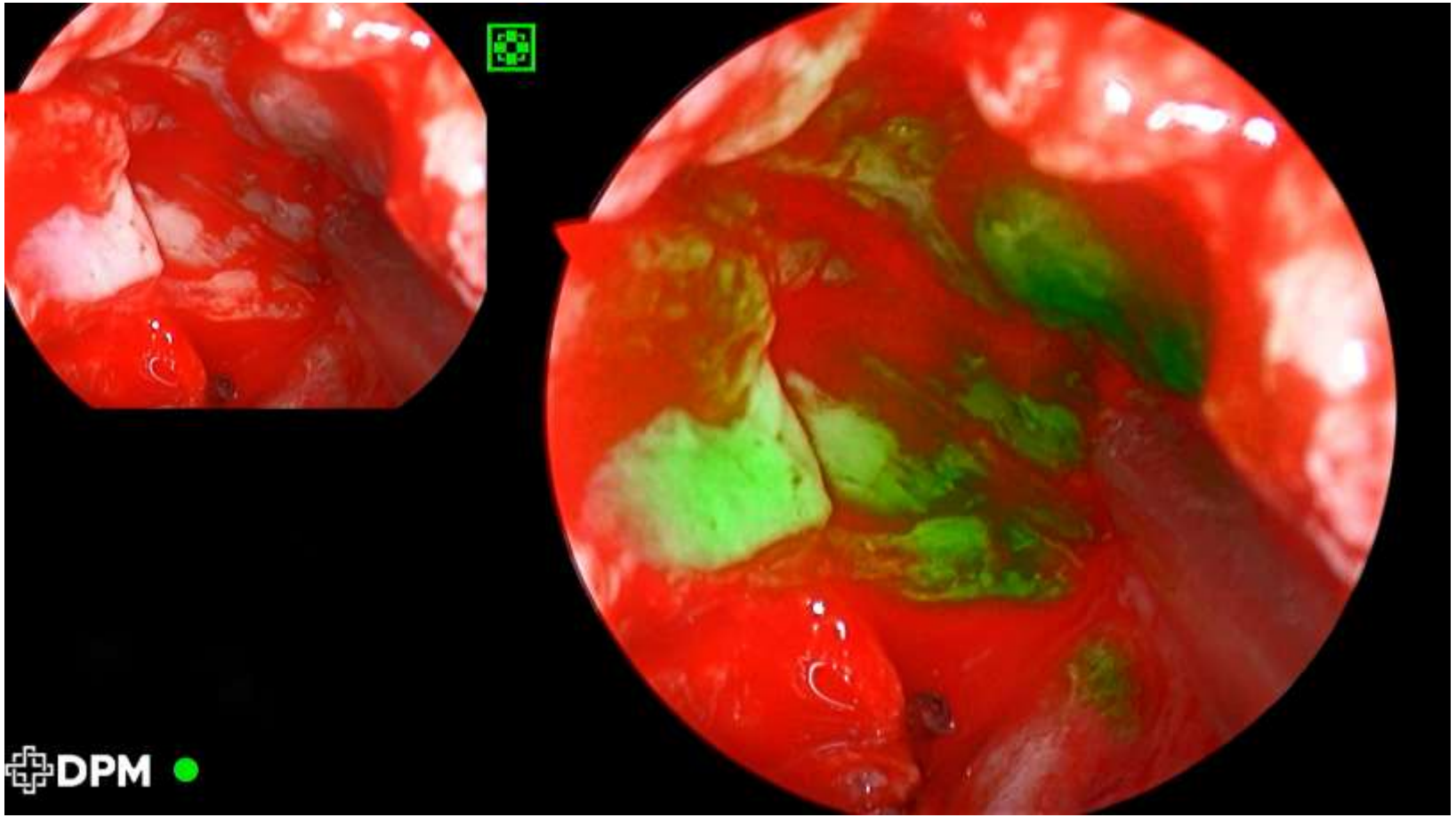

Case 30

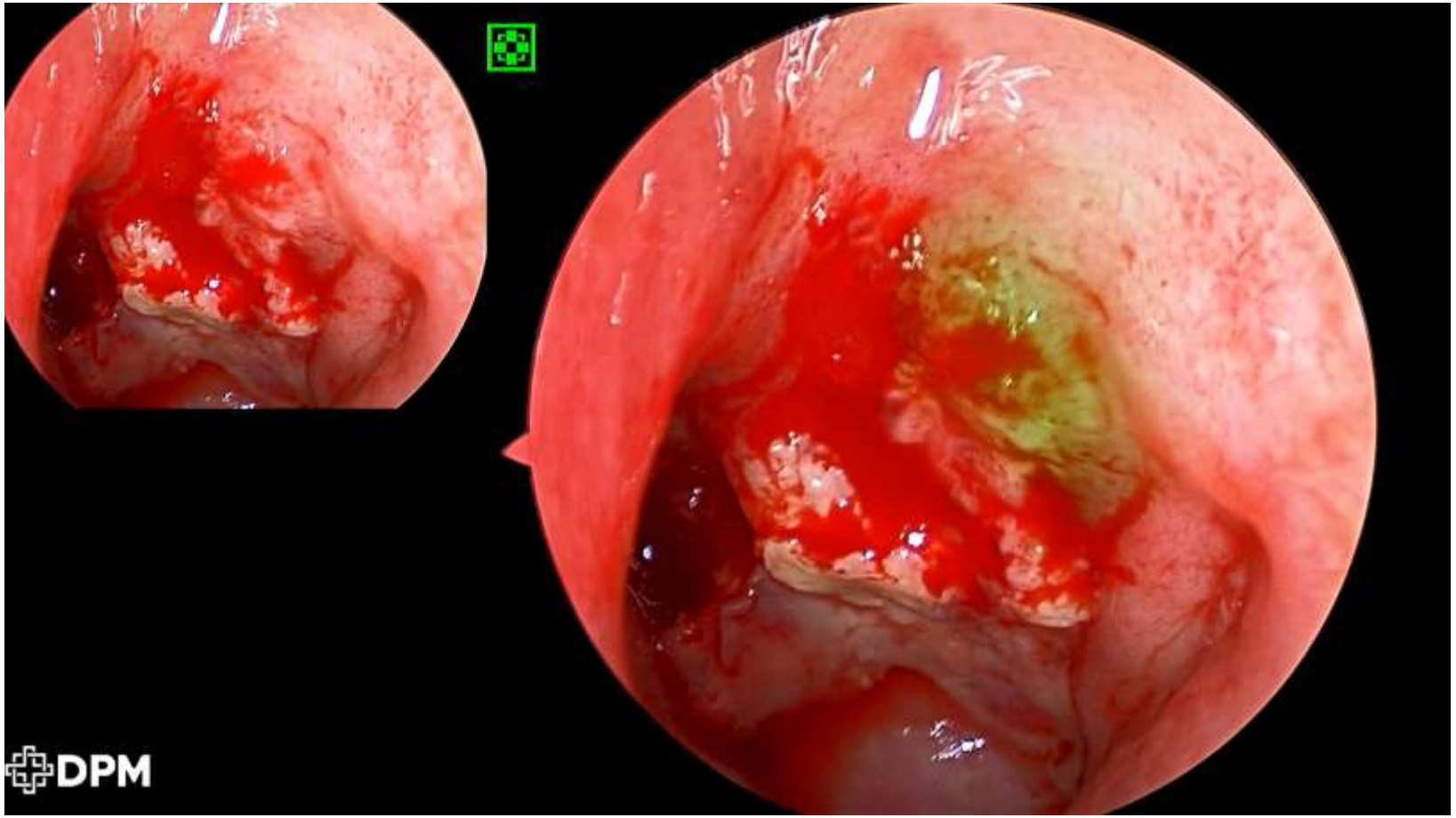

Case 31

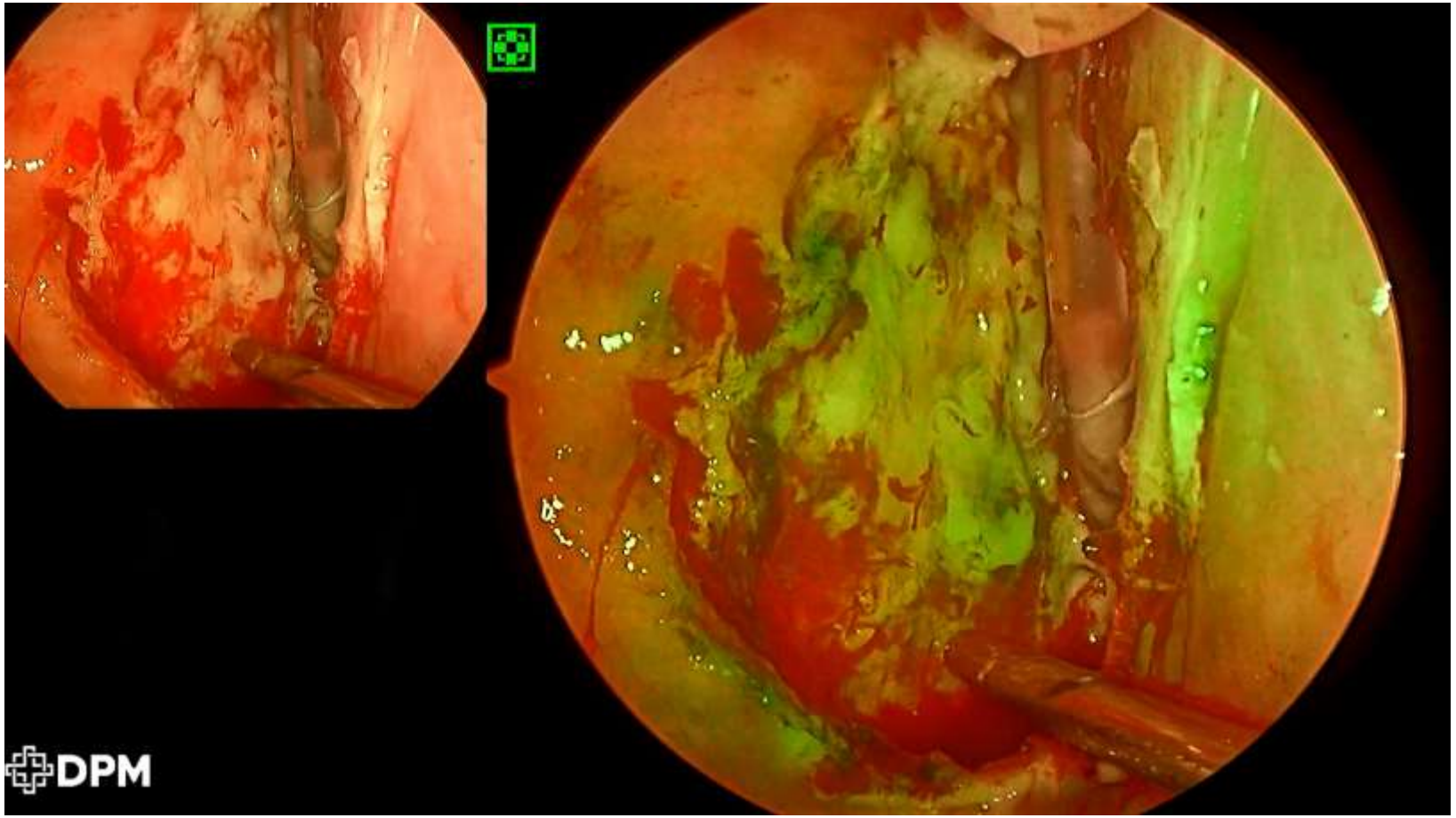

Case 32

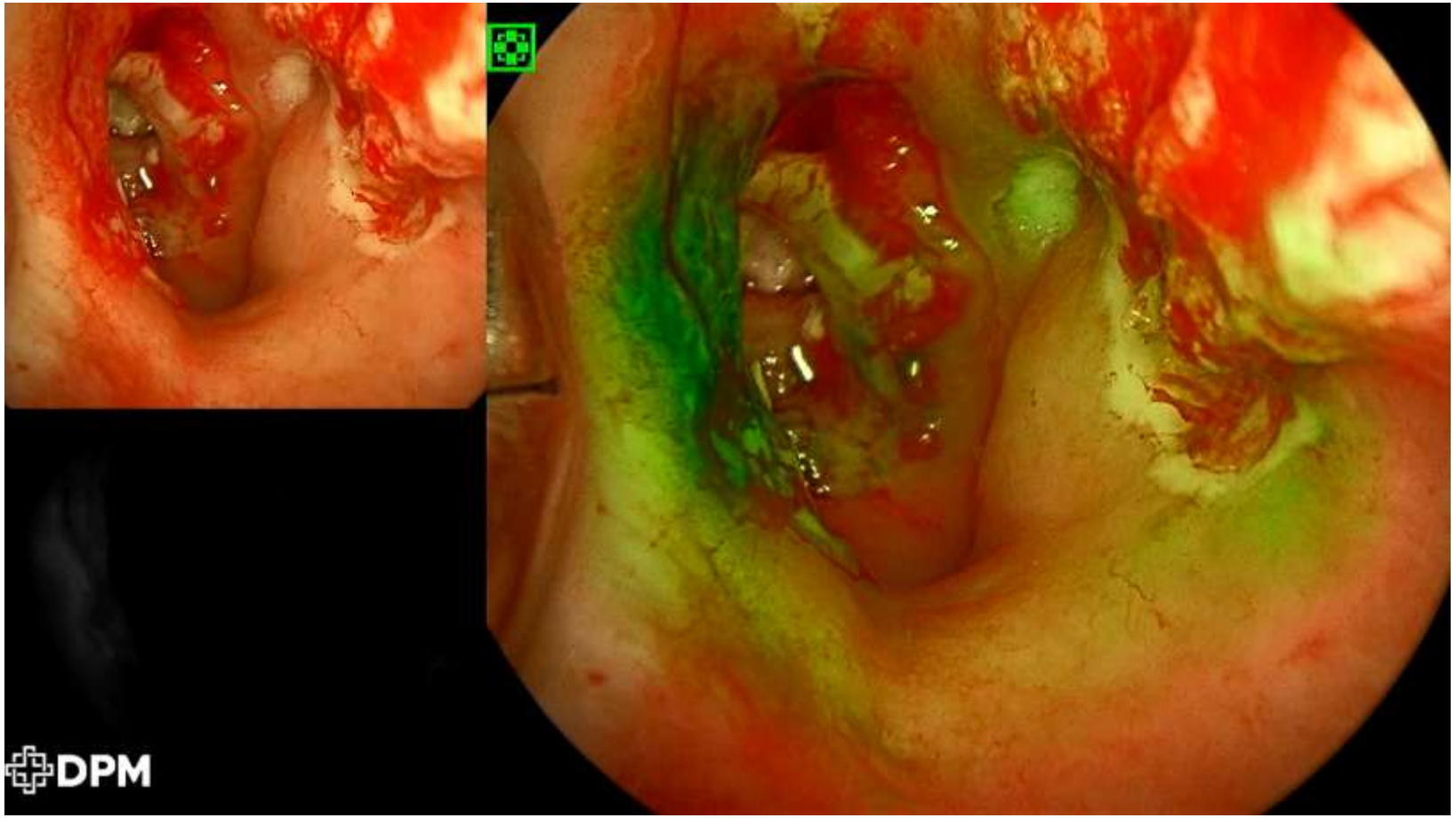

Case 33

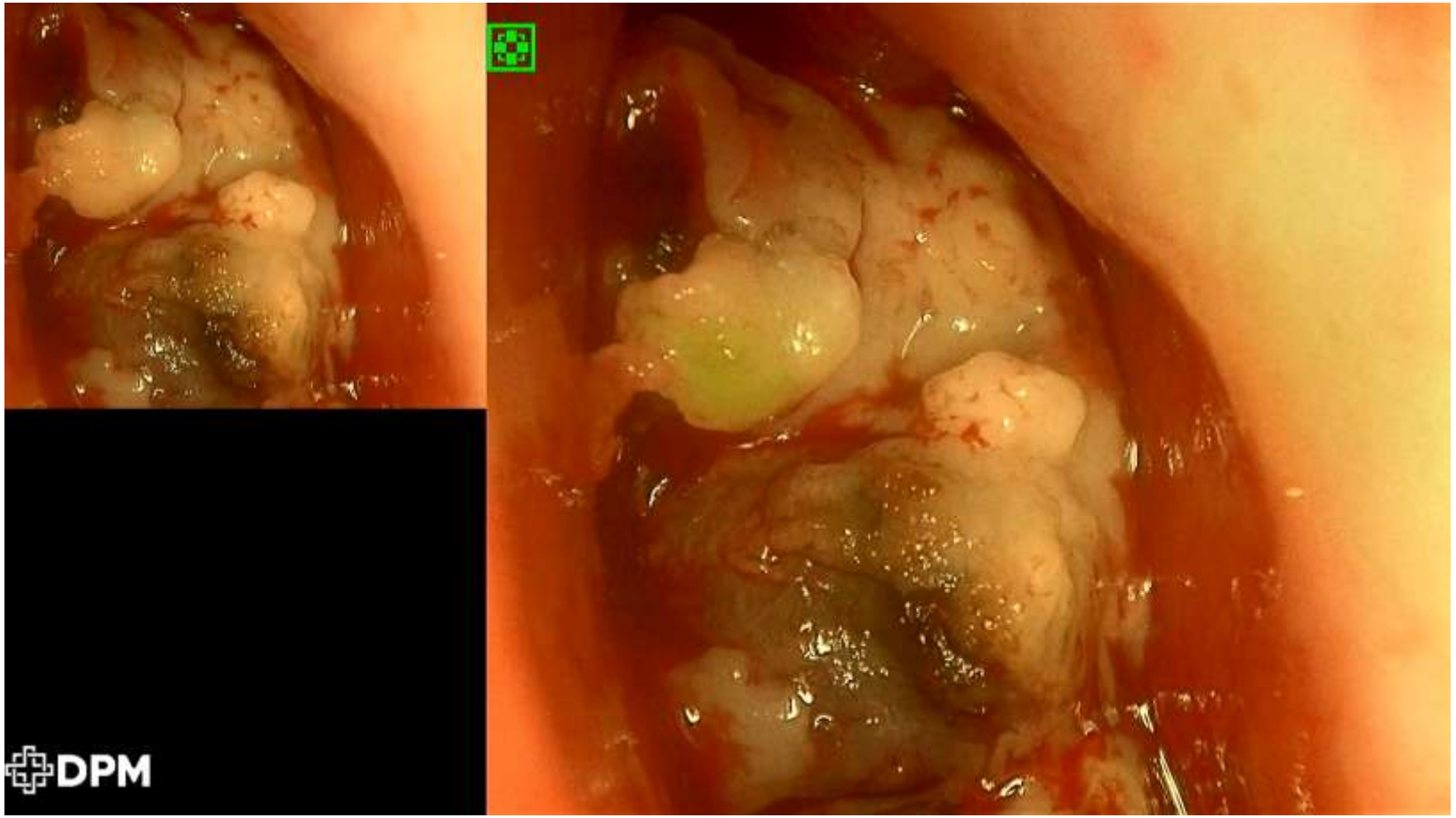

Case 34

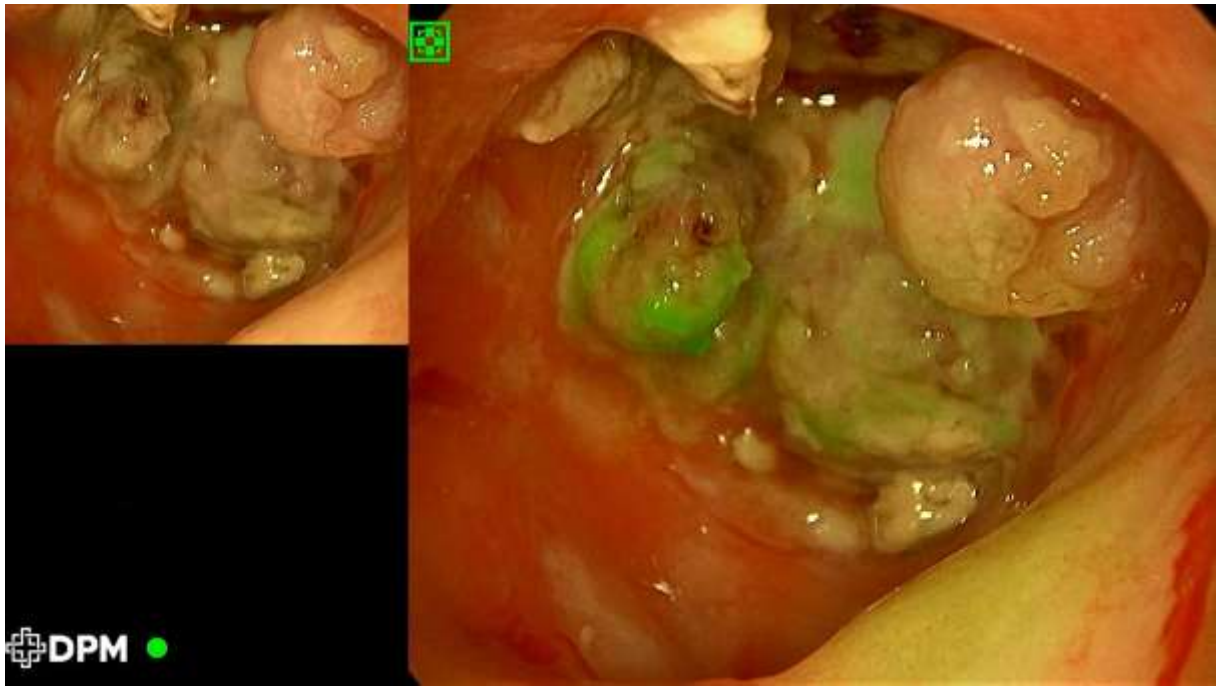

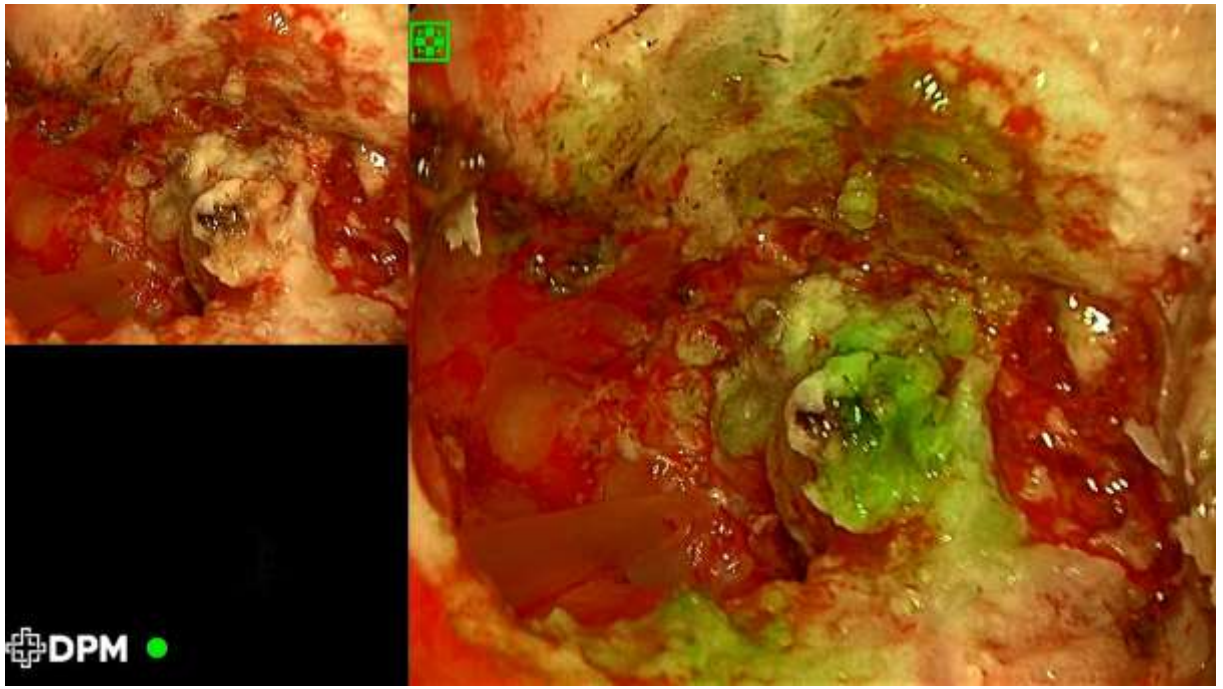

Case 35

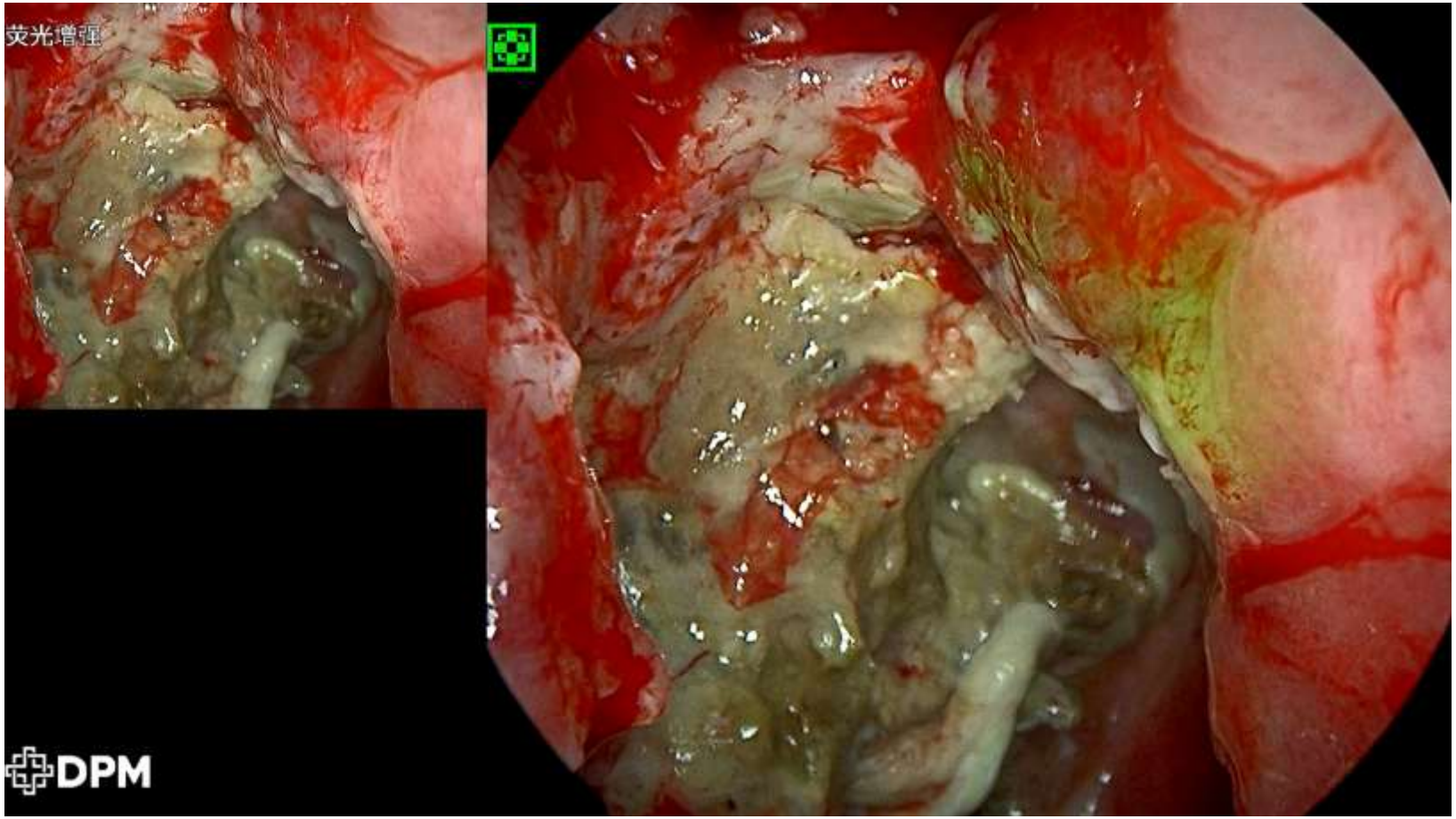

Case 36

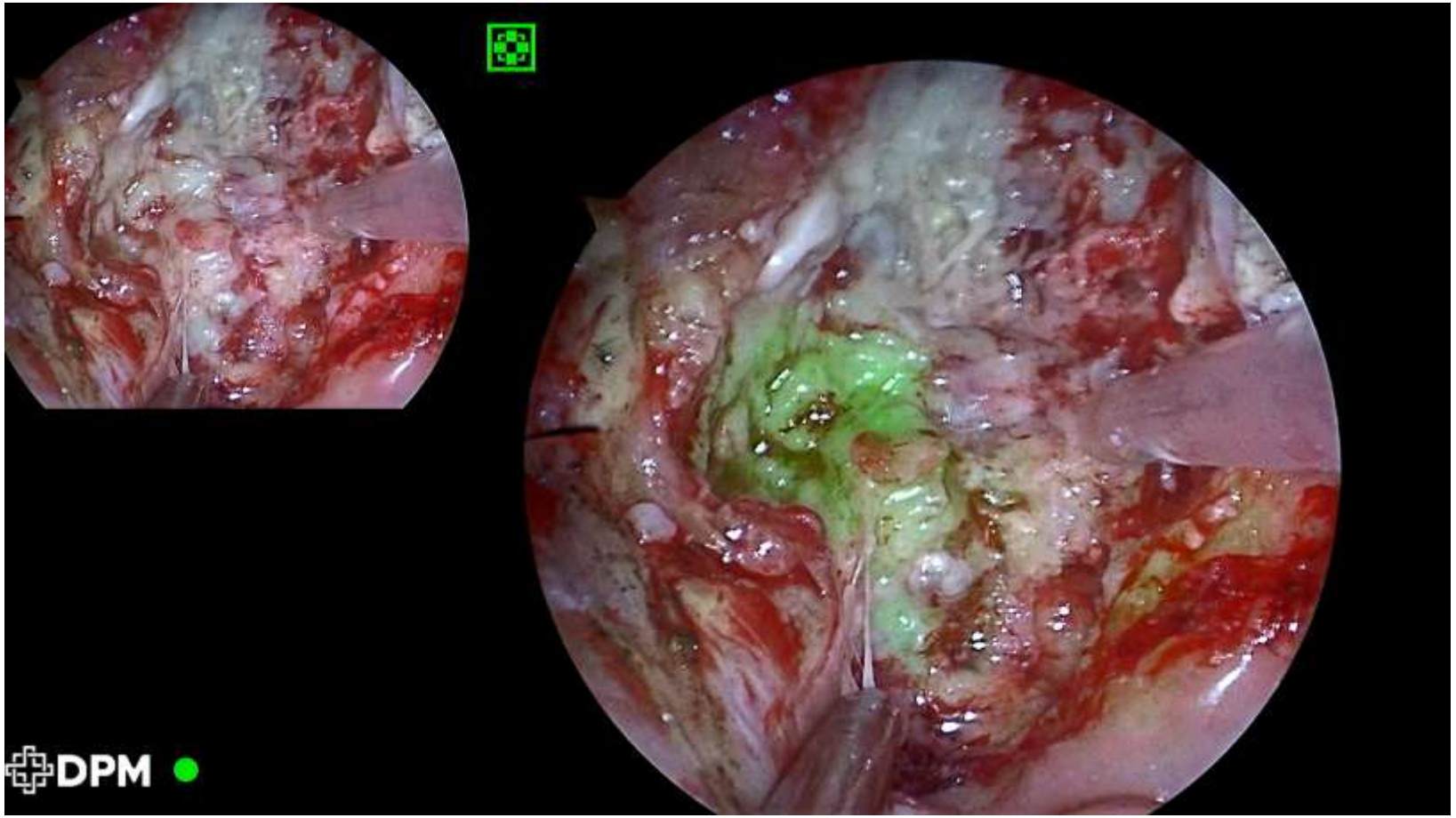

Case 38

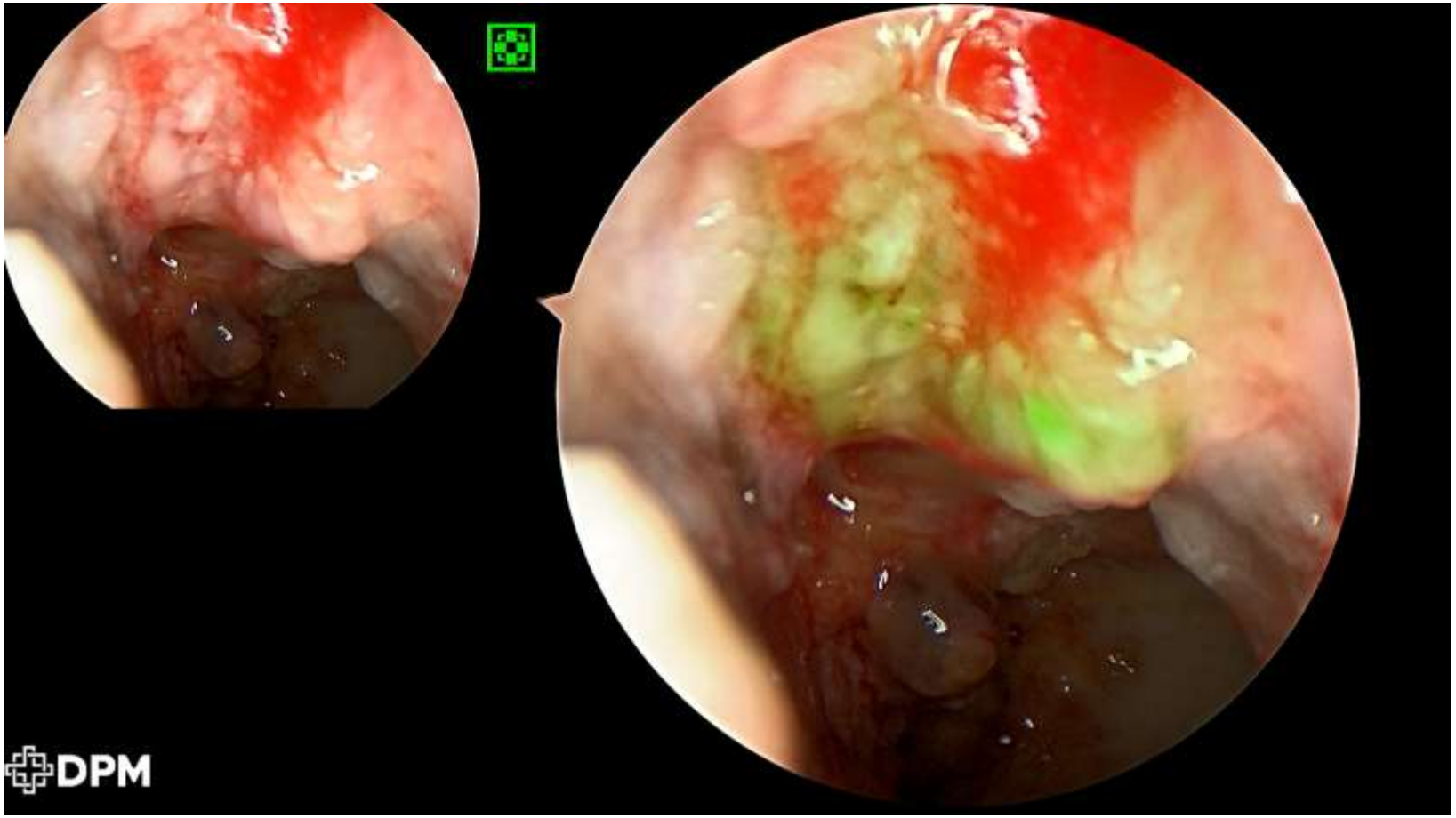

Case 39

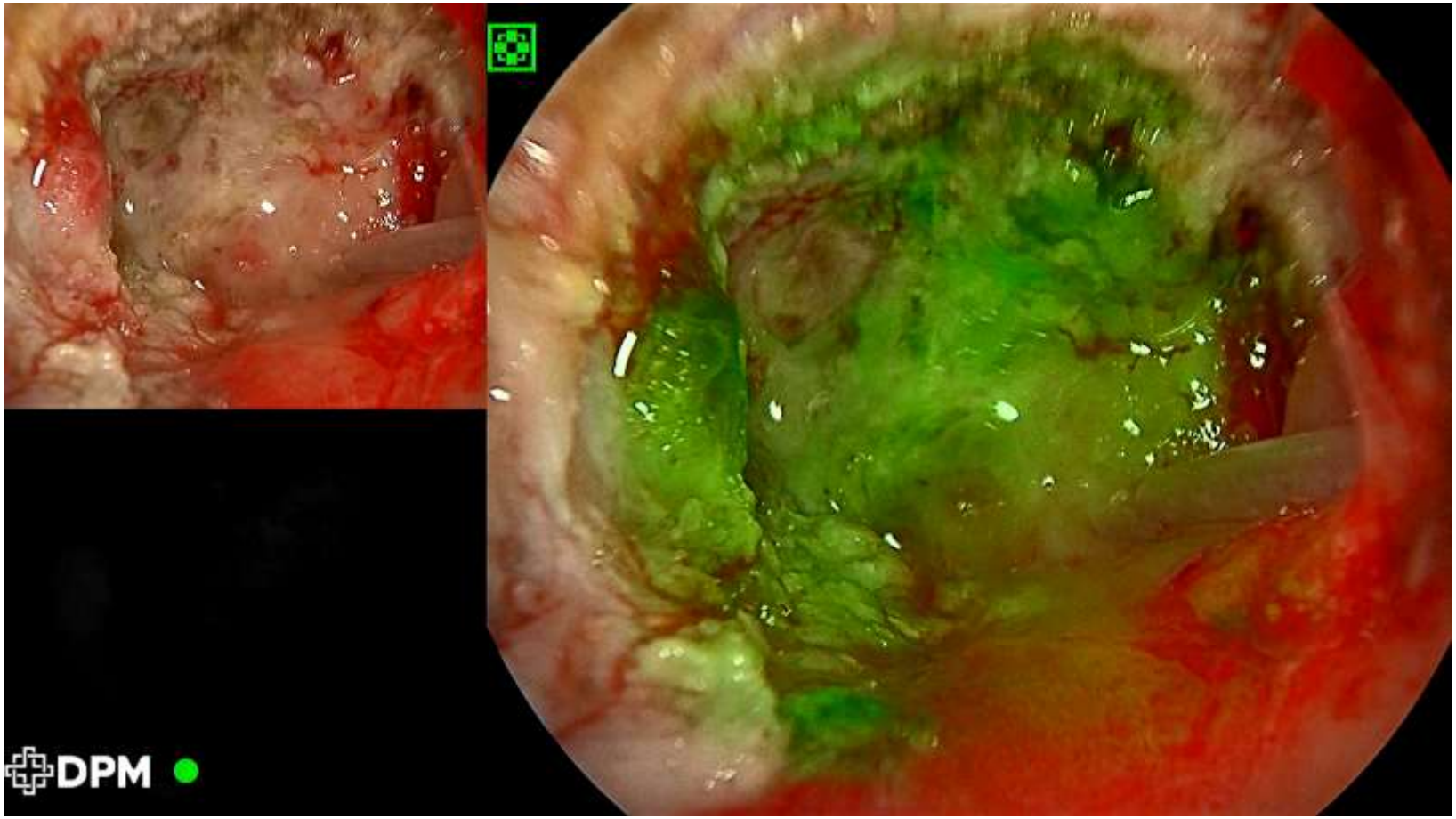

Case 40

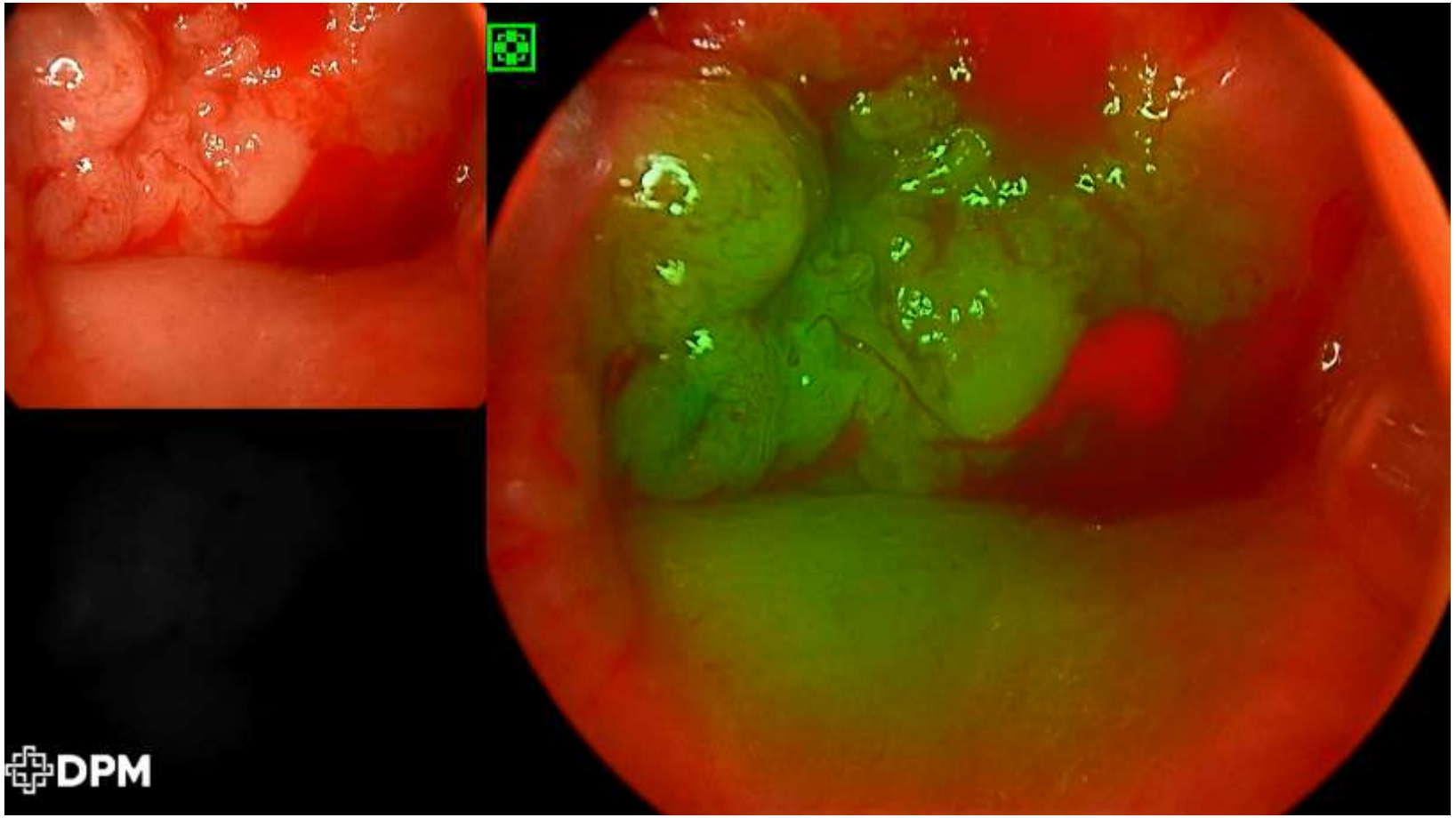

Case 41

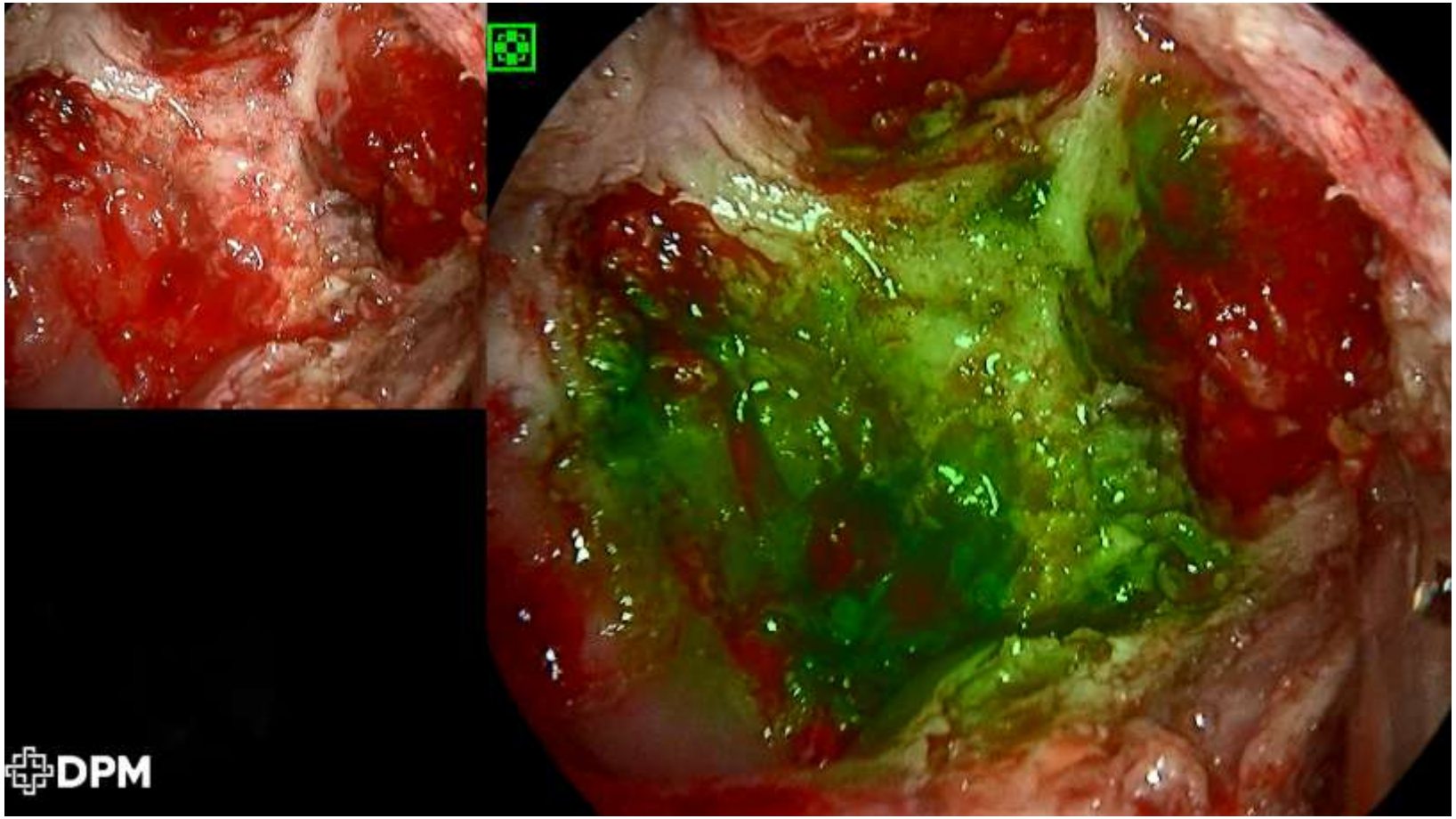

Case 42

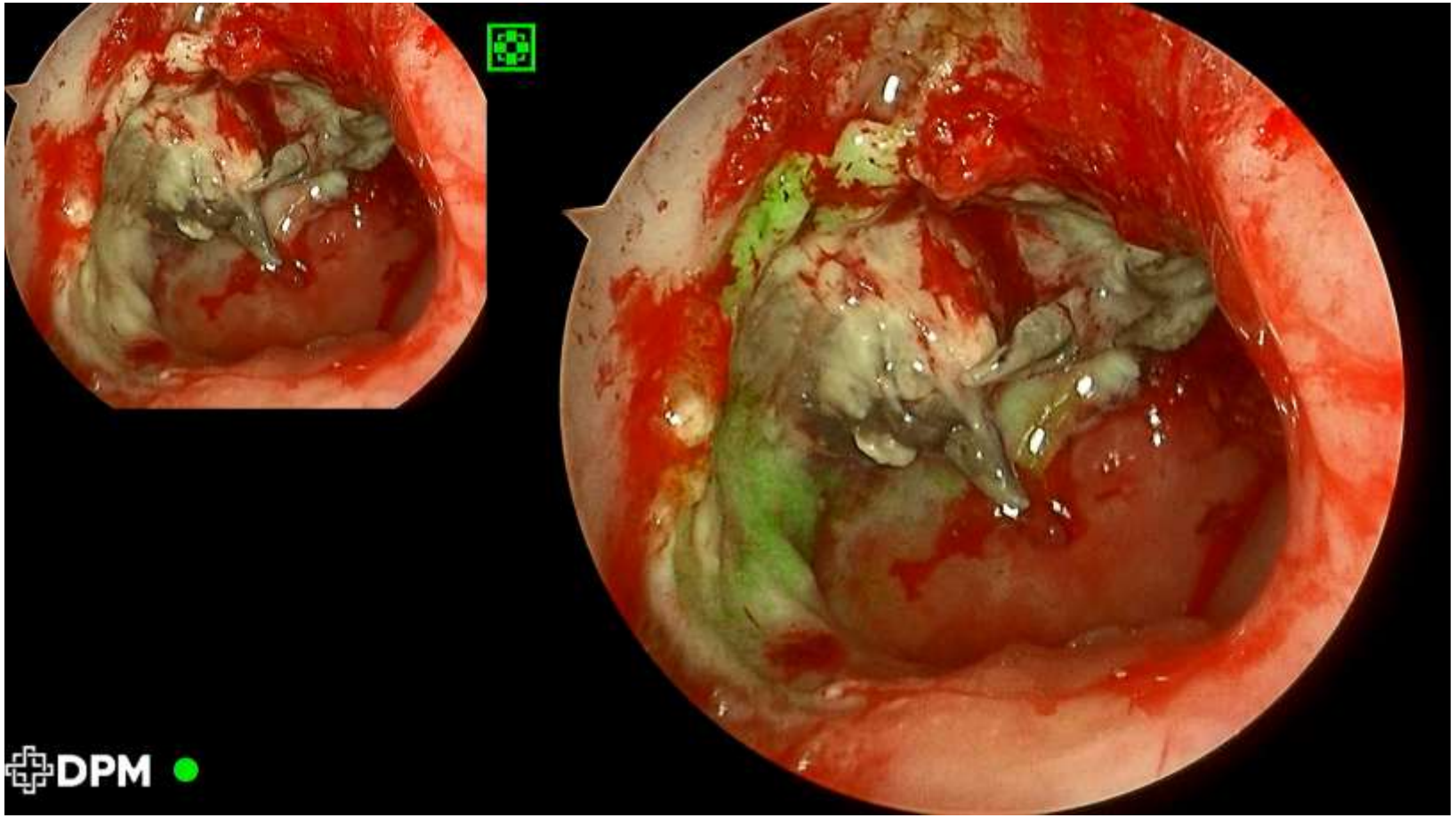

Case 43

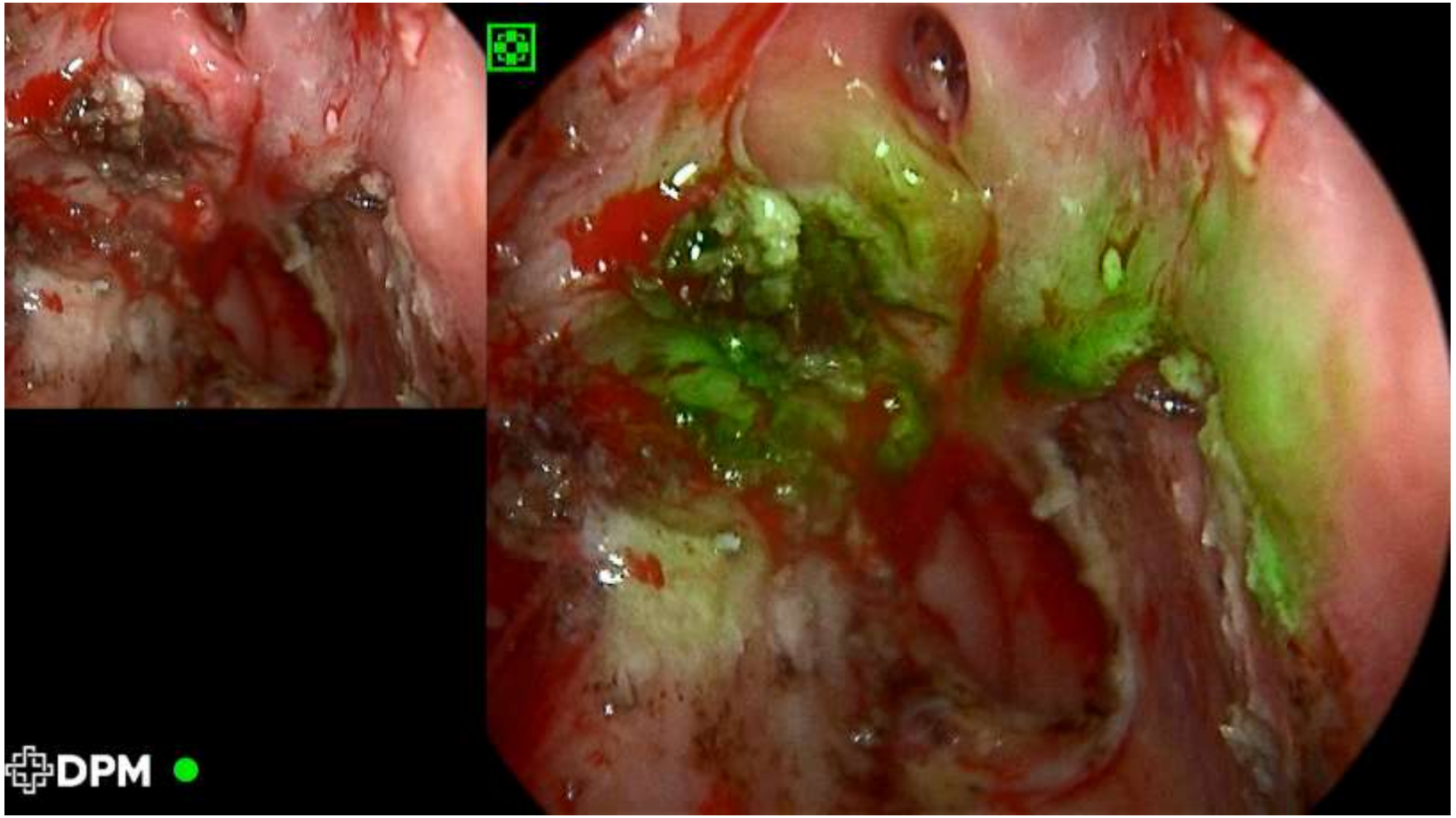

Case 44

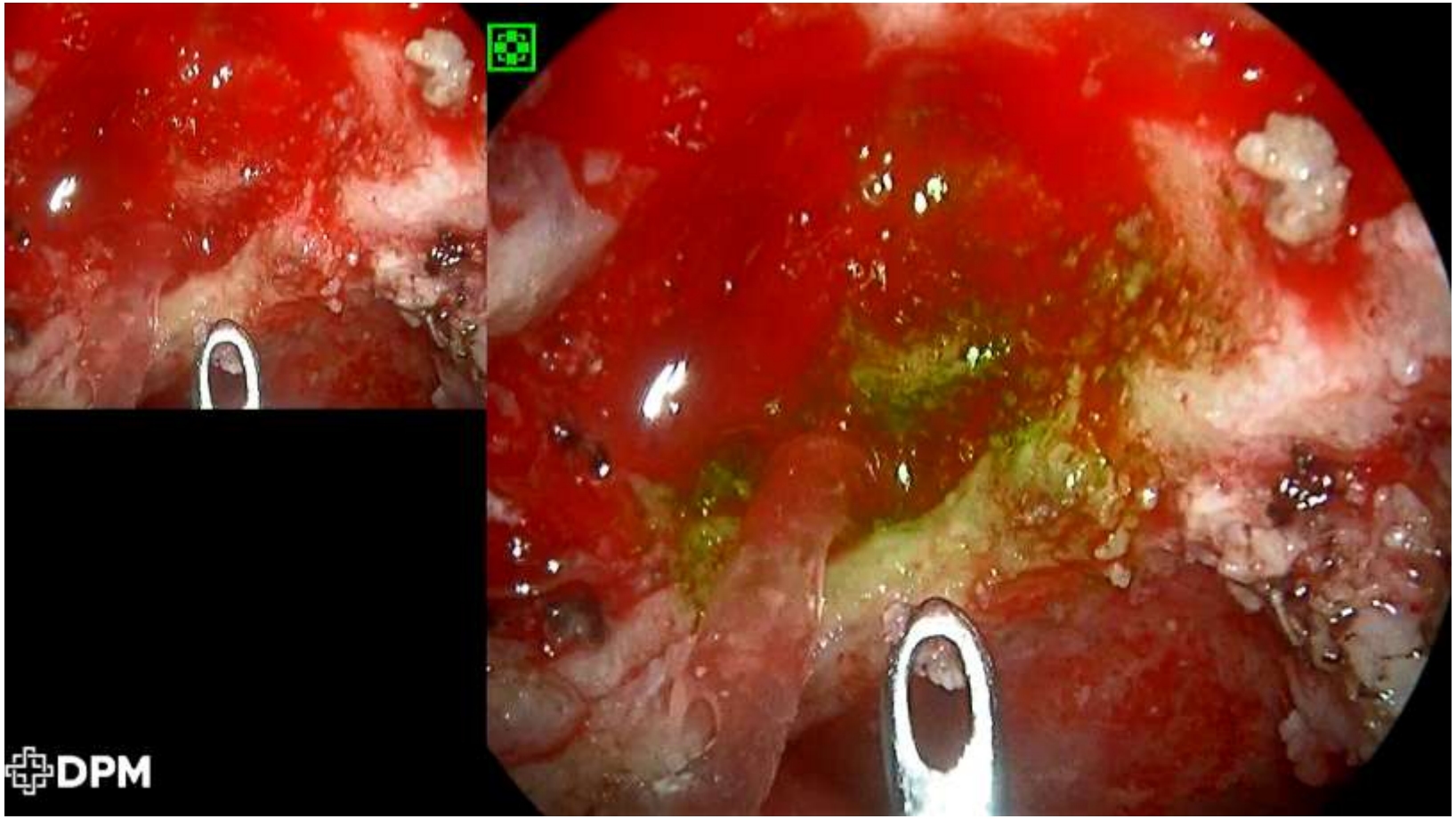

Case 45

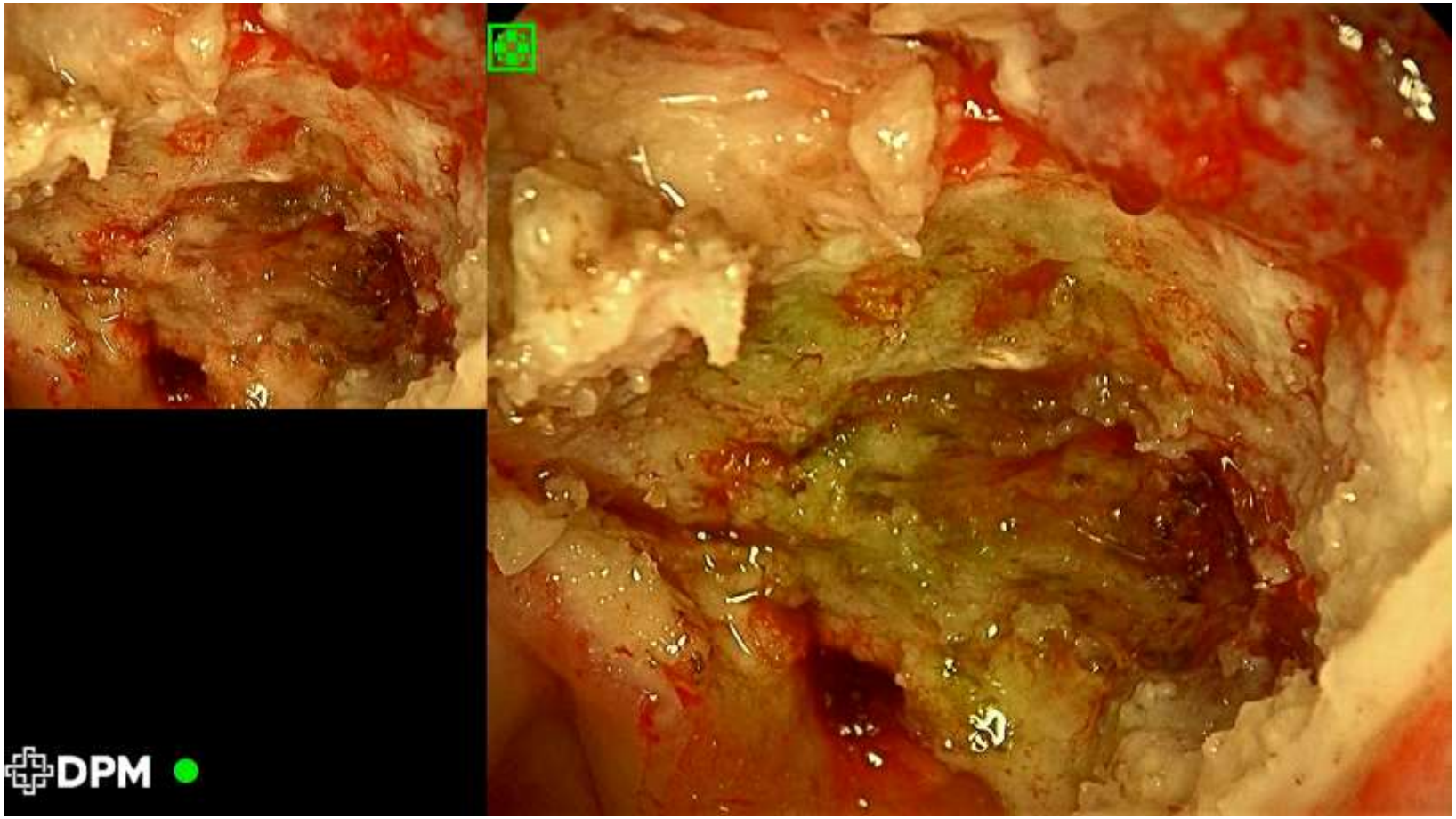

Case46